Orogenic to postorogenic (1.20–1.15 Ga) magmatism in the Adirondack Lowlands and Frontenac terrane, southern Grenville Province, USA and Canada

William H. Peck[1], Bruce W. Selleck[1], Martin S. Wong[1], Jeffrey R. Chiarenzelli[2], Karen S. Harpp[1], Kurt Hollocher[3], Jade Star Lackey[4], Joseph Catalano[3], Sean P. Regan[2], and Andrew Stocker[4]

[1]*Department of Geology, Colgate University, Hamilton, New York 13346, USA*
[2]*Department of Geology, St. Lawrence University, Canton, New York 13617, USA*
[3]*Department of Geology, Union College, Schenectady, New York 12308, USA*
[4]*Department of Geology, Pomona College, Claremont, California 91711, USA*

ABSTRACT

Magmatism in the southern Grenville Province records a collisional and postcollisional history during the period 1.20–1.15 Ga in the Adirondack Lowlands (New York State, USA) and the Frontenac terrane (Ontario, Canada). The 1.20 Ga bimodal Antwerp-Rossie suite of the Adirondack Lowlands was produced by subduction in the Trans-Adirondack backarc basin. This was followed by intrusion of the 1.18 Ga alkalic to calc-alkalic Hermon granite, which may have been generated by melting of metasomatized mantle during collision of the Adirondack Lowlands and Frontenac terrane during the Shawinigan orogeny. The Hyde School gneiss plutons intruded the Adirondack Lowlands at 1.17 Ga, and Rockport granite intruded into the Adirondack Lowlands and Frontenac terrane, stitching the Black Lake shear zone, which marks the boundary between these terranes. Subsequent extensional collapse and lithospheric delamination caused voluminous anorthosite-mangerite-charnockite-granite plutonism. In the Frontenac terrane, this event is represented by the 1.18–1.15 Ga Frontenac suite, which is composed predominately of ferroan granitoids produced from melting of the lower crust by underplating mafic magmas. The Edwardsville, Honey Hill, and Beaver Creek plutons are newly recognized members of this suite in the Adirondack Lowlands. High oxygen isotope ratios of this suite in the central Frontenac terrane and western Adirondack Lowlands point to the presence of underthrust altered oceanic rocks in the lower crust. Oxygen isotopes of the Frontenac suite in both terranes preclude its derivation from mantle melts alone.

INTRODUCTION

The allochthonous monocyclic belt of the southwestern Grenville Province (New York State, USA and Ontario, Canada) consists predominately of plutonic suites that intruded supracrustal country rocks during the period 1.3–1.0 Ga (Rivers et al., 1989). The dominant plutonic component in the allochthonous monocyclic belt is the voluminous anorthosite-mangerite-charnockite-granite (AMCG) suite, which was emplaced ca. 1.15 Ga (Doig 1991; McLelland et al., 2004). Tectonic models for generation of the AMCG suite once called upon incipient rifting or plume activity in an otherwise anorogenic setting (Ashwal, 1993), but with refined geochronology in the 1990s, it became clear that several pulses of AMCG magmatism followed compressional orogenesis. Grenville AMCG suites are now generally interpreted to be the result of postcollisional collapse and crustal delamination causing mafic magma underplating and melting of the lower crust, giving rise to anorthosites and ferroan (A-type) granitoids of the AMCG suite, respectively (McLelland et al., 1996; Corrigan and Hanmer, 1997). This contribution focuses on magmatism in the Adirondack Lowlands (New York) and Frontenac terrane (Ontario), an area that has a magmatic record of 1.20 Ga subduction, 1.17 Ga convergence, and 1.17–1.15 Ga postorogenic intrusion of gabbros and ferroan granitoids. We compare the Frontenac suite in Ontario and correlative plutons in the Adirondack Lowlands. The Frontenac and Adirondack Lowlands terranes are interpreted to have been sutured together along the Black Lake shear zone (BLSZ) during the 1.19–1.14 Ga Shawinigan orogeny (Wong et al., 2011). Magmatic suites ca. 1.17 Ga or younger stitch this boundary, allowing differences in lower crustal composition and magma sources to be characterized (cf. Peck et al., 2004).

GEOLOGIC SETTING

The Adirondack Lowlands and Frontenac terranes are part of the allochthonous monocyclic belt of Rivers et al. (1989), comprising juvenile Mesoproterozoic rocks accreted to (or formed on) the margin of Laurentia (Fig. 1). Terranes in the allochthonous monocyclic belt are interpreted as a collage of arcs, basins, and continental fragments accreted to Laurentia ca. 1.2 Ga (e.g., Carr et al., 2000), or as a 1.4–1.2 Ga Andean-type margin with associated backarc environments (e.g., Hanmer et al., 2000). Regional metamorphism during the collisional 1.19–1.14 Ga Shawinigan orogeny reached 640–680 °C in the Adirondack Lowlands and 700–750 °C in the Frontenac terrane, both at ~6–7 kbar (Streepey et al., 1997). The Adirondack Lowlands (Fig. 2) are dominated by metasedimentary rocks that include metapelites with minor associated intrusive and volcanic rocks, calcitic and dolomitic marbles, siliceous metacarbonates, evaporites, and metasediment-hosted sulfide ore deposits (Carl et al., 1990), as well as minor distal arc volcanic and or volcaniclastic rocks (Popple Hill gneiss) and quartzite (Chiarenzelli et al., 2011a).

Evidence from Nd isotopes has allowed the separation of juvenile and evolved Grenville rocks in the Central Metasedimentary Belt of Ontario, and suggests that a backarc failed rift

Geosphere; December 2013; v. 9; no. 6; p. 1637–1663; doi:10.1130/GES00879.1; 13 figures; 8 tables.
Received 31 October 2012 ♦ Revision received 28 May 2013 ♦ Accepted 28 August 2013 ♦ Published online 11 October 2013

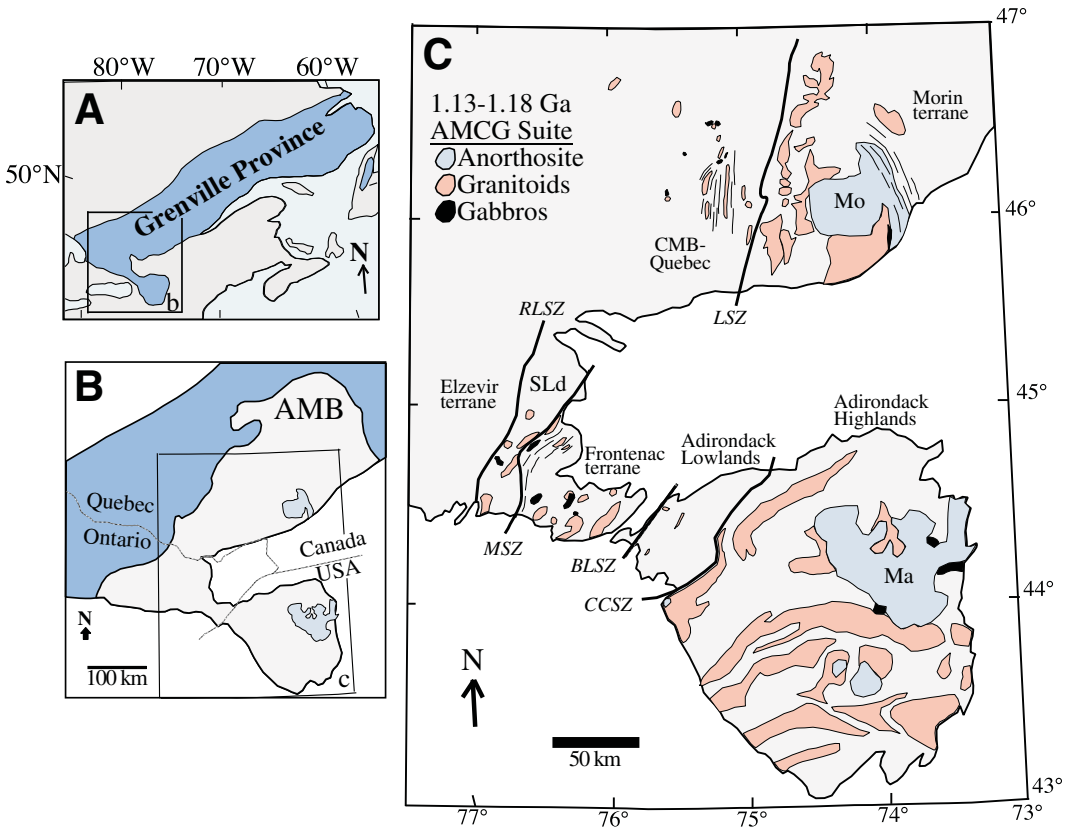

Figure 1. (A) Location of the study area within the Grenville Province. (B) Location map and subdivisions of the allochthonous monocyclic belt (AMB) of the Grenville Province (after Peck et al., 2004, and references therein). (C) Detail of B. AMCG—anorthosite-mangerite-charnockite-granite, CMB-Quebec—Central Metasedimentary Belt of Quebec, SLd—Sharbot Lake domain of the Elzevir terrane, Ma—Marcy anorthosite massif, Mo—Morin anorthosite massif, CCSZ—Carthage-Colton shear zone, BLSZ—Black Lake shear zone, LSZ—Labele shear zone, MSZ—Maberly shear zone, RLSZ—Robertson Lake shear zone. Thin line clusters indicate zones of penetrative deformation.

began to open ca. 1.3 Ga (Fig. 3; Dickin and McNutt, 2007). Rifting proceeded to the extent that sedimentary rocks, including sandstones and limestones, blanketed most of the area, although rifting eventually ceased, and arc rocks of the Elzevir terrane were added to the southeast margin of Laurentia during the ca. 1.2 Ga Elzevirian orogeny (McLelland et al., 2010a). In Chiarenzelli et al. (2010a), it was proposed that a similar basin called the Trans-Adirondack backarc basin formed to the east (present coordinates) of the Central Metasedimentary Belt at the same time. This interpretation is largely based on the recognition of oceanic crust and upper mantle in the Adirondack Lowlands and preservation of metasedimentary rocks in contact with oceanic material. In the Adirondack Lowlands the metasedimentary assemblage includes an apparently intact sequence, the "lower marble" (an informal designation used in the Adirondack Lowlands to designate a widespread unit of calcite marble with intercalated quartzite that may be stratigraphically distinct from the "upper marble"; see Weiner et al., 1984), Popple Hill gneiss, and "upper marble" tectonostratigraphic units. These rocks have recently been interpreted to represent rift to drift to closure of the Trans-Adirondack basin (Chiarenzelli et al., 2011b). The oldest mafic members of the bimodal Antwerp-Rossie metaigneous suite are intrusive into this sequence, and provide a minimum age for its deposition (older than 1.2 Ga).

Geochronology data indicate that sedimentary rocks in the Adirondacks were deposited between ca. 1.28 and 1.22 Ga (Chiarenzelli et al., 2011a). There is evidence of initial convergence and the imminent collapse of the basin preserved in the sedimentary sequence while protoliths of the "upper marble" were deposited, ca. 1.22 Ga. Sequences of stratiform Zn-Pb exhalative rocks and evaporite units are preserved. Carbonates hosting the Zn-Pb exhalatives were deposited after the evaporites, perhaps indicating migration of hydrothermal, metal-rich brines following pulses of convergence and uplift. This episodic uplift may have isolated the region from the open ocean and led to precipitation of evaporites. Eventual closure and collision occurred, and deformation, metamorphism, and magmatism stepped outward from the Adirondack Lowlands toward intrusive centers in the central Adirondack Highlands.

The Adirondack Lowlands terrane was intruded by two (now metamorphosed) plutonic suites that are not present in the Frontenac terrane: the bimodal ca. 1.20 Ga calc-alkaline Antwerp-Rossie suite (Wasteneys et al., 1999; Chiarenzelli et al., 2010b), and the ca. 1.18 Ga (Heumann et al., 2006) alkali to calc-alkaline Hermon granite (Carl and deLorraine, 1997). The Adirondack Lowlands also contain the distinctive ca. 1.17 Ga domical Hyde School leucogranite to tonalitic gneiss bodies (McLelland et al., 1991; Wasteneys et al., 1999). The last major plutonic event recorded in the Adirondack Lowlands includes the ca. 1.16 Ga Edwardsville pluton (McLelland et al., 1993) and several correlative syenitic bodies (Buddington, 1934). These plutonic suites are all penetratively deformed to some degree, and were followed by younger scattered, relatively undeformed (and undated) red granites (Buddington, 1934).

The Frontenac terrane contains quartzite, pelitic rocks, marble, and siliceous metacarbonate rocks, but lacks metavolcanic rocks. Intrusive activity in the terrane was dominated by monzonite, syenite, granite, and gabbro plutons of the A-type 1.18–1.15 Ga Frontenac suite (Marcantonio et al., 1990; Davidson and van Breemen, 2000). The heterogeneously deformed, ca. 1.17 Ga Rockport granite (van Breemen and Davidson, 1988; Wasteneys et al., 1999) is contemporaneous with the Frontenac suite and syntectonically intruded the BLSZ.

The BLSZ is a northeast–trending zone of high strain that separates the distinct rock types and metamorphic histories of the Frontenac terrane and Adirondack Lowlands (Mezger et al., 1993; Wong et al., 2011). The BLSZ is

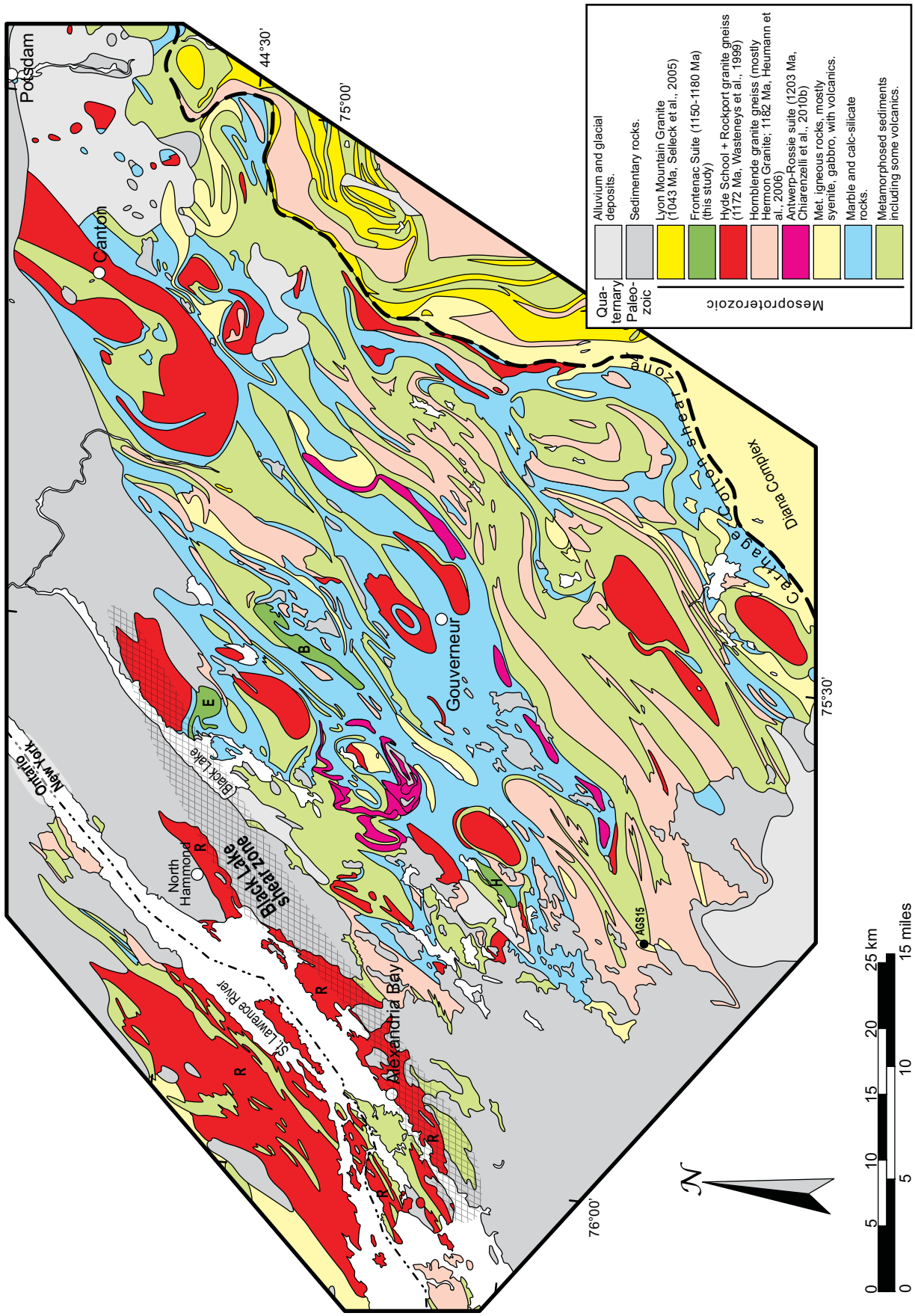

Figure 2. Geology of the Adirondack Lowlands compiled from Fisher et al. (1970), Carl et al. (1990), Wasteneys et al. (1999), Selleck et al. (2005), and Wong et al. (2011). E—Edwardsville pluton, R—Rockport granite, H—Honey Hill pluton, B—Beaver Creek pluton.

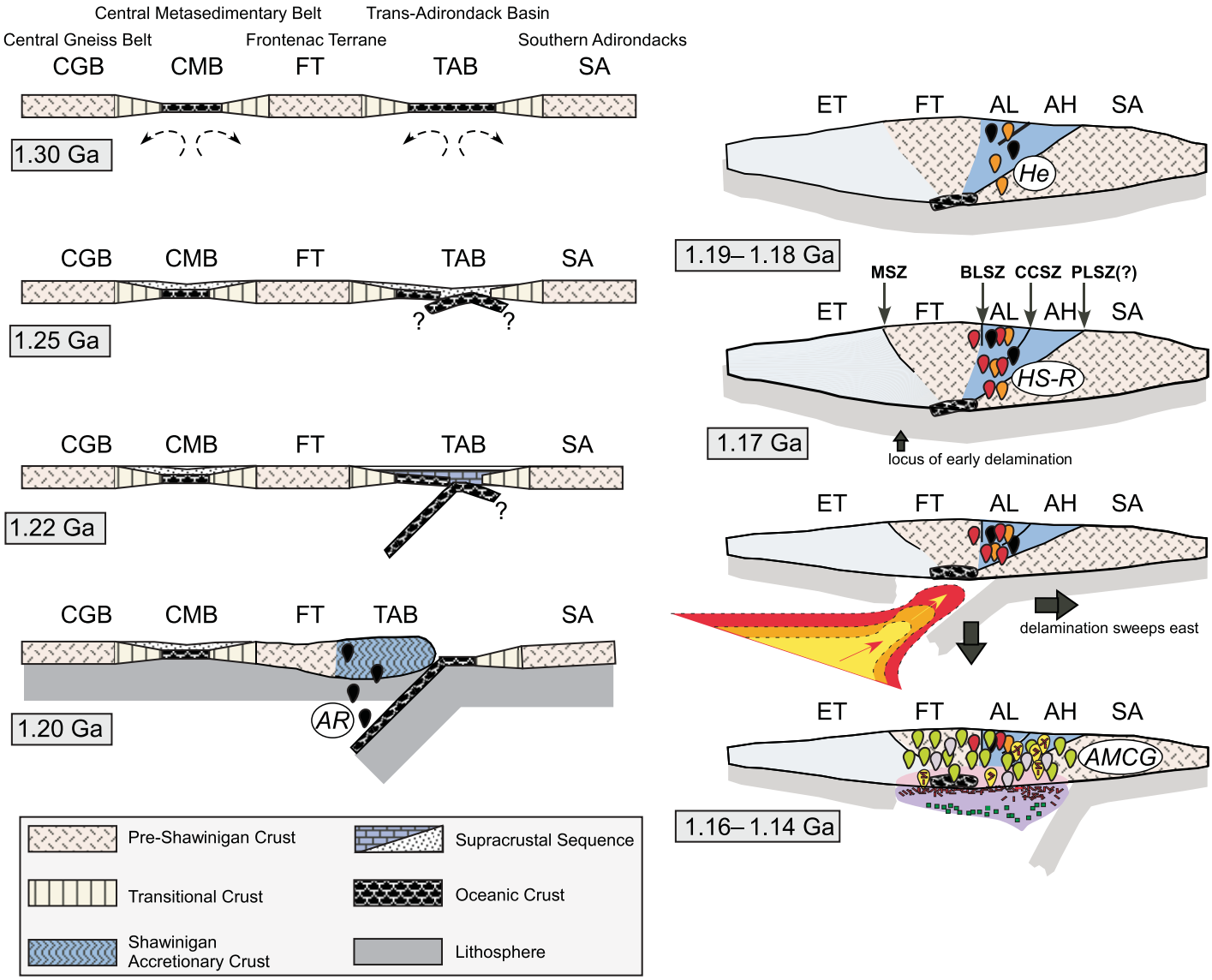

Figure 3. Summary of tectonic evolution of the Adirondack Lowlands and Frontenac terrane from 1.30 to 1.14 Ga (after Chiarenzelli et al., 2010b; Regan et al., 2011). Subduction and other details of the ca. 1.19–1.14 Ga Shawinigan orogeny are not specified in the Central Metasedimentary Belt (CMB.) CGB—Central Gneiss Belt, ET—Elzevir terrane, FT—Frontenac terrane, TAB—Trans-Adirondack basin, SA—southern Adirondacks, AH—Adirondack Highlands, AL—Adirondack Lowlands, MSZ—Maberly shear zone, BLSZ—Black Lake shear zone, CCSZ—Carthage-Colton shear zone, PLSZ—Piseco Lake shear zone, AR—Antwerp-Rossie suite (black plutons), He—Hermon granite gneiss (orange plutons), HS-R—Hyde School gneiss and Rockport granite (red plutons), AMCG—anorthosite-mangerite-charnockite-granite (and gabbro) plutons, including the Frontenac suite (anorthosites are yellow, granitoids are green, and gabbros are purple). Dark purple is underplating mafic magma, and dark pink is melted lower crust. In panels after 1.20 Ga (right), light blue is undifferentiated crust in the Elzevir terrane and dark blue shows the amalgamated Trans-Adirondack basin (Adirondack Lowlands and Adirondack Highlands). For these panels, the nature of the pre-Ottawan lower crust is necessarily schematic.

predominantly subvertical and accommodated northwest-directed shortening and perhaps transpressional deformation. Timing constraints indicate that deformation was ongoing during intrusion of the ca. 1.17 Ga Rockport granite and was complete no later than ca. 1.10 Ga and possibly by ca. 1.16 Ga. The nature and timing of this deformation is consistent with other studies in this part of the Adirondack Lowlands (e.g., Baird and Shrady, 2011). Wong et al. (2011) interpret the BLSZ as accommodating the tectonic juxtaposition of the Frontenac and Adirondack Lowlands terranes during the Shawinigan orogeny, associated with closure of the backarc basin that formed at the edge of Laurentia at 1.28–1.22 Ga (Chiarenzelli et al., 2010b).

METHODS

Major and trace element geochemistry was determined from a range of samples of recognized 1.18–1.15 Ga magmatic suites including the Hermon granite, Rockport granite, Hyde School gneiss, and the Frontenac suite. One focus of the sampling strategy was a compari-

son of the Edwardsville pluton in the Adirondack Lowlands and plutons of the Frontenac suite in Ontario. In addition, the Edwardsville and Honey Hill plutons were sampled for U-Pb zircon geochronology.

Representative samples (n = 10) of the Hermon granite were selected for major and trace element geochemistry using X-ray fluorescence (XRF) for major elements and inductively coupled plasma–mass spectrometry (ICP-MS) for trace elements at the ACME Analytical Laboratories (Vancouver, British Columbia, Canada; http://acmelab.com/services/). Major element analyses for other plutons (51 samples) were performed at Colgate University (Hamilton, New York) using a Philips PW2404 XRF (see Chiarenzelli et al., 2010b). Trace elements from five samples from the Edwardsville pluton were determined by ICP-MS at ACME Analytical Laboratories, and by XRF on pressed-powder pellets at Colgate University (Chiarenzelli et al., 2010b). Trace elements for 20 samples from Rockport and Hyde School granite gneisses were determined using methods described in Hollocher et al. (2007). Trace elements for 16 samples from the Frontenac suite were determined with an Agilent HP4500 ICP-MS (Harpp et al., 2005). Zr, Nb, Hf, Ta, Th, and U are not reported for some samples from the Frontenac suite in Ontario and from the Edwardsville pluton that had anomalously low measured concentrations, presumably due to incomplete dissolution of zircon and/or oxides. New major and trace element compositions (Tables 1–6) match well with published results. The geochemical and petrological characteristics of the various suites are discussed in the following.

Samples of the Edwardsville pluton selected for geochronology were processed at Pomona College using a UA Bico Pulverizer, a Gemeni GT60 MK.2 shaking table, methylene iodide, and a Frantz Isodynamic separator. Zircon crystals were hand-picked from concentrates using a binocular microscope and were screened for cracks and alteration. Samples were mounted in epoxy with standards, polished to expose cross-sections of grain interiors, gold coated, and examined using backscattered electron and cathodoluminescence (CL) imaging prior to and following ion microprobe analysis. U-Pb geochronology of zircon was conducted at the U.S. Geological Survey–Stanford University SUMAC SHRIMP-RG laboratory (Stanford USGS Micro Analysis Center, sensitive high-resolution ion microprobe–reverse geometry) using standard procedures (e.g., Premo et al., 2008, and references therein). Analyses used an O^{2-} primary beam that produced ~20-µm-diameter × 1–2-µm-deep spots (Table 7). Sample analyses were interspersed with analyses of the VP-10 standard, and data reduction was performed using the Squid and Isoplot programs (Ludwig, 2001, 2008).

Oxygen isotopes in zircon were analyzed by laser fluorination using a 35W CO_2 laser at the University of Oregon (Table 8; Bindeman et al., 2008). Bulk zircon samples were 1.0–2.3 mg, evolved oxygen was analyzed as CO_2 using a Finnigan MAT 253 mass spectrometer, and analyses were standardized to UWG2 (Valley et al., 1995). Zircon was analyzed because its refractory nature allows oxygen isotope ratios of magmas to be calculated even in polymetamorphic igneous rocks (Valley et al., 2005). Zircons from the analyzed magmatic suites retain igneous ages and only have rare inherited cores or later overgrowths (Davidson and van Breemen, 2000; Hamilton et al., 2004). These features are volumetrically minor, so have only a small potential impact on the measured oxygen isotope ratio of whole zircons.

RESULTS AND DISCUSSION

1203 Ma Antwerp-Rossie Metaigneous Suite

The Antwerp-Rossie metaigneous suite is a bimodal suite of deformed granitic, granodioritic, and dioritic orthogneisses. It is the oldest of the plutonic suites recognized as intrusive into the supracrustal sequence exposed in the Adirondack Lowlands, southeast of the BLSZ. The geology of these rocks was described in Chiarenzelli et al. (2010b), and additional geochemical analyses and discussion are in Carl and deLorraine (1997). We also utilize data from metamorphosed mafic intrusive bodies that include the Pleasant Lake metagabbro, metagabbros near Harrisville, the Balmat metadiorite, and the Split Rock metadiorite (see Carl, 2000), which are correlative members of this suite (Chiarenzelli et al., 2011b). These mafic bodies share common geochemical characteristics with the Antwerp-Rossie suite, and some span the 52.5–62.5 wt% SiO_2 compositional gap present in most members of this suite (Chiarenzelli et al., 2010b). The crystallization age of this suite is 1203 ± 13.6 Ma based on SHRIMP-RG analysis of zircon (Chiarenzelli et al., 2010b).

The Antwerp-Rossie suite is characterized by a high-K geochemistry and is metaluminous (Fig. 4). According to the terminology of Frost and Frost (2008), this suite is magnesian and calc-alkalic (Figs. 4B, 4C). The Antwerp-Rossie suite has broadly arc-like trace element contents with high Cs, Pb, La, and Nd, and low Nb, Ta, P, Ti, and Zr (Fig. 4G). Rare earth elements (REE) show a light (L) REE enrichment (La_n/Sm_n = 1.8–7.2) and range from nearly flat to strongly depleted heavy (H) REE patterns (Sm_n/Yb_n = 1.9–14.3), implying a range of sources from garnet free to garnet rich (Fig. 4I). In general, the most felsic members of the suite (Antwerp granitoids, SiO_2 > 62.5%) have higher La_n/Sm_n (average, av. = 4.8) and Sm_n/Yb_n (av. = 7.0) ratios than the mafic rocks (Rossie metadiorites, SiO_2 < 52.5%) (av. = 3.0 and 4.3, respectively).

Neodymium model ages (T_{DM}; depleted mantle) for the Antwerp-Rossie suite range from 1.3 to 1.6 Ga, with ε_{Nd} values of 1.5–5.4 at 1.2 Ga (Chiarenzelli et al., 2010b). The suite is interpreted to have formed during closure of a backarc basin between the Frontenac terrane and the southern Adirondack Highlands during the Shawinigan orogeny at 1.2 Ga (Fig. 4), based on its location at the northwest margin of the Adirondack Lowlands and its geochemistry.

Although the geochemical traits of the Antwerp-Rossie suite and, to a lesser extent, the Hermon granite, discussed in the following, strongly suggest the influence of subduction-related melts, the tectonic setting of subduction has only recently been better understood. Evidence suggests that the southeast margin of Laurentia (present coordinates) was an Andean-type margin for much of the time leading up to the ca. 1.07 Ga Ottawan orogeny (Wasteneys et al., 1999; Hanmer et al., 2000; Chiarenzelli et al., 2010a). In post-Shawinigan plutonic rocks (Frontenac suite) in the Frontenac terrane, highly elevated $\delta^{18}O$ values of zircon were found (to 15‰; Peck et al., 2004), compared to global average $\delta^{18}O$ values for zircon from granitic rocks (Valley et al., 2005). This enrichment ends near the BLSZ, a structure (Fig. 2) that has been proposed to be the boundary between the Frontenac terrane and the Adirondack Lowlands (Wasteneys et al., 1999; Chiarenzelli et al., 2010b; Wong et al., 2011). T_{DM} Nd model ages calculated for the Antwerp-Rossie suite increase westward toward the BLSZ to a maximum of 1.6 Ga along the boundary (Chiarenzelli et al., 2010a). In addition, the BLSZ serves as the western boundary of the Antwerp-Rossie and Hermon granite suites. These constraints help establish the location of the boundary between the Frontenac and Adirondack Lowlands, the polarity of pre-Shawinigan subduction, and allow the influence of subducted sediments and/or hydrothermal altered oceanic crust in the source region to be evaluated.

Fragments of oceanic crust and upper mantle rocks have recently been identified in the Adirondack Lowlands (Chiarenzelli et al., 2010b, 2011b) implying the presence of pre-Shawinigan oceanic crust south of the BLSZ. The ultramafic Pyrites complex consists of hydrothermally altered crust that shows subduction-related geochemical trends (with negative Nb, Ta, P, and Zr, and positive Cs, Pb, La,

TABLE 1. MAJOR AND TRACE ELEMENT DATA FOR HERMON GRANITE SAMPLES, ADIRONDACK LOWLANDS, NEW YORK STATE, USA

	AL-09-9	AL-09-11	AL-09-20	AL-09-27	AL-09-29	AL-09-30	AL-09-34	AL-09-35	AL-09-55A	AL-09-55b
Lat (°N)	44.3826	44.3878	44.5036	44.2609	44.3169	44.3099	44.4405	44.4372	44.5780	44.5720
Long (°W)	75.2946	75.3176	75.3581	75.7623	75.2070	75.2130	75.2538	75.2595	74.8732	75.8590
SiO_2	60.20	61.85	55.84	69.74	66.86	65.95	65.71	62.27	65.53	69.05
Al_2O_3	16.42	17.03	16.88	15.42	15.06	15.59	16.1	16.52	14.71	14.97
Fe_2O_3	7.36	5.16	6.25	2.06	3.99	3.82	3.99	5.16	5.95	2.63
MgO	1.96	1.88	3.60	0.69	0.60	0.58	1.58	1.85	1.02	0.75
CaO	3.57	3.05	4.11	0.52	2.11	1.79	1.78	3.37	2.97	1.28
Na_2O	3.63	3.75	3.51	4.04	3.93	4.12	3.66	3.86	3.37	3.08
K_2O	4.04	4.48	6.22	5.47	5.8	5.69	4.95	3.62	3.93	5.72
TiO_2	1.00	0.80	0.89	0.48	0.73	0.75	0.65	0.83	0.91	0.52
P_2O_5	0.34	0.31	0.55	0.16	0.22	0.24	0.27	0.31	0.39	0.15
MnO	0.09	0.05	0.09	0.01	0.07	0.05	0.03	0.05	0.09	0.04
Cr_2O_3	0.002	<0.002	0.005	<0.002	<0.002	<0.002	<0.002	<0.002	<0.002	<0.002
LOI	1.00	1.30	1.50	1.10	0.30	1.00	0.90	1.80	0.80	1.50
Total	99.61	99.66	99.45	99.69	99.67	99.58	99.62	99.64	99.67	99.69
Be	2	2	3	4	2	2	2	2	1	1
Sc	12	8	11	4	5	5	7	9	11	5
V	86	69	127	25	<8	<8	50	66	41	16
Co	27.6	22.4	22.2	74.3	32.7	52.7	45.8	24.5	18.9	33.4
Ni	6.3	5.2	12.7	2.0	1.2	1.3	3.7	5.0	3.2	1.6
Cu	10.8	4.8	3.9	0.6	1.6	1.4	8.9	4.4	8.7	1.8
Zn	104	63	46	19	60	28	59	80	98	33
Ga	22.5	22.1	19.4	21.5	20.9	21.3	20.1	21.1	21.1	16.0
Rb	108.1	94.3	155.7	145	110.8	104.9	120.1	107.7	75.5	96.1
Sr	476.8	456.3	1144.3	357.1	341.2	355.3	315.2	423.4	264.7	243.0
Y	39.9	25.5	35.5	11.3	37.2	36.6	31.7	24.0	47.0	16.9
Zr	364.2	329.6	410.6	279.8	621.3	678.6	403.5	396.9	474.1	304.4
Nb	16.4	12.2	17.7	24.2	21.4	27.8	20.4	14.2	19.9	17.1
Mo	0.6	0.5	0.3	0.7	0.9	0.8	0.5	0.4	0.9	0.6
Sn	5	2	3	2	2	2	3	2	<1	<1
Cs	1.9	1.6	3.0	1.5	0.7	0.2	1.9	2.6	0.4	0.8
Ba	1184	1250	1536	705	1041	1085	1024	1049	1134	1156
La	74.4	55.7	89.0	72.7	36.4	32.1	65.9	47.9	43.9	79.2
Ce	155.8	120.9	203.7	133.0	79.1	71.0	150.7	103.2	100.6	164.6
Pr	18.47	14.65	24.35	15.49	10.29	9.74	17.87	12.36	13.57	19.52
Nd	74	58.7	96.9	54.4	43.3	41.5	68.2	47.5	58.4	71.6
Sm	12.13	8.99	15.08	7.22	8.40	7.98	11.80	8.05	11.72	9.68
Eu	2.65	2.48	3.39	1.42	2.56	2.53	2.23	2.12	3.41	2.44
Gd	9.53	6.84	10.58	4.16	7.32	7.26	8.52	6.24	10.72	5.79
Tb	1.45	0.99	1.46	0.54	1.22	1.21	1.22	0.90	1.66	0.73
Dy	7.30	4.86	6.93	2.34	6.70	6.64	6.13	4.57	9.18	3.52
Ho	1.29	0.87	1.10	0.37	1.29	1.30	1.06	0.79	1.69	0.57
Er	3.62	2.37	3.06	0.99	3.83	3.73	2.96	2.31	4.68	1.66
Tm	0.52	0.34	0.45	0.14	0.55	0.54	0.42	0.31	0.65	0.24
Yb	3.04	1.99	2.85	0.86	3.65	3.40	2.55	1.98	3.96	1.46
Lu	0.4	0.30	0.41	0.13	0.55	0.51	0.35	0.30	0.58	0.22
Hf	9.9	8.9	10.9	8.3	15.6	17.0	11.4	10.2	13.0	8.6
Ta	4.3	3.1	2.2	11.7	7.2	12.6	7.7	4.8	3.0	8.3
W	221.8	212.6	85.2	520.0	263.8	507.7	367.1	256.6	164.4	395.2
Pb	3.4	1.4	2.8	1.6	2.7	2.5	1.4	1.6	1.7	4.0
Th	8.9	7.0	16.7	24.5	3.1	1.2	15.7	6.6	0.7	17.8
U	1.0	1.1	4.5	3.3	1.3	0.5	1.4	1.5	0.6	1.0

Note: Oxides are weight percents, elements are parts per million. LOI—loss on ignition.

TABLE 2. MAJOR AND TRACE ELEMENT DATA FOR HYDE SCHOOL GNEISS SAMPLES, ADIRONDACK LOWLANDS, NEW YORK STATE, USA

	JC24	JC28	JC30	JC34	JC36	JC39	JC41
Lat (°N)	44.3441	44.3685	44.4595	44.4199	44.4502	44.5262	44.5144
Long (°W)	75.4790	75.4697	75.5559	75.8070	75.5437	75.5727	75.5727
SiO_2	74.76	75.62	75.74	73.96	72.06	74.13	75.43
Al_2O_3	12.99	14.00	10.94	13.89	14.60	15.17	13.65
Fe_2O_3	2.94	1.53	5.23	2.83	2.07	0.65	1.31
MgO	0.50	0.10	0.90	0.20	0.70	0.10	0.10
CaO	1.05	0.68	0.80	1.18	0.94	1.00	0.83
Na_2O	3.87	5.78	2.93	5.13	4.27	6.52	5.27
K_2O	4.28	2.89	3.67	3.05	5.03	2.24	3.55
TiO_2	0.22	0.15	0.38	0.43	0.33	0.35	0.07
P_2O_5	0.04	0.02	0.02	0.04	0.09	0.10	0.01
MnO	0.02	0.02	0.01	0.01	0.02	<0.01	0.02
LOI	0.92	0.58	0.91	0.59	0.43	2.12	0.38
Total	101.59	101.37	101.53	101.31	100.54	102.38	100.62
Li	7.1	4.93	8.6	2.50	2.09	7.9	3.50
Be	1.37	4.72	1.52	1.95	2.17	1.01	1.50
Sc	5.4	4.84	2.13	5.5	0.68	2.28	1.55
V	12.1	5.9	18.4	3.29	0.140	8.1	2.32
Cr	2.01	0.33	1.72	0.13	0.09	0.54	0.52
Co	2.41	0.98	3.87	1.76	1.13	2.65	1.46
Ni	2.16	0.76	6.0	1.30	0.26	2.96	0.98
Cu	1.0	0.73	23	2.4	0.48	4.2	4.1
Zn	11.8	22.9	15.4	2.34	47.5	19.1	37
Ga	19.1	22.7	27.1	22.1	27.1	18.2	22.4
Rb	75	45.9	66	39.1	138	124	88
Sr	71	60	66	135	28.2	306	49
Y	41.6	38.9	68	28.2	135	24.0	44.8
Zr	409	397	955	486	522	317	387
Nb	7.5	18.9	7.7	14.8	21.1	8.2	9.9
Mo	0.02	0.13	0.15	0.32	0.05	0.06	0.08
Sn	1.60	3.6	4.7	3.2	6.6	2.9	3.0
Cs	0.167	0.230	0.163	0.052	0.096	0.79	0.156
Ba	613	206	249	589	71	999	543
La	29.3	37.4	63.8	45.7	48.7	65.1	26.6
Ce	66	109	143	104	117	131	63
Pr	8.4	10.2	19.1	15.0	16.0	16.3	7.7
Nd	35.3	39.6	77.8	64.0	66.5	60.9	31.2
Sm	7.6	8.0	16.0	13.0	17.9	10.9	7.2
Eu	1.17	0.97	2.67	2.49	0.86	2.09	1.22
Gd	7.0	6.8	13.9	9.5	19.3	8.3	7.0
Tb	1.13	1.13	2.00	1.08	3.61	1.07	1.27
Dy	7.1	7.2	11.8	5.4	23.7	5.3	8.4
Ho	1.50	1.51	2.43	1.03	5.05	0.89	1.80
Er	4.37	4.41	7.0	3.04	14.5	2.09	5.3
Tm	0.70	0.71	1.09	0.51	2.22	0.272	0.84
Yb	4.69	4.83	7.4	3.58	13.7	1.69	5.6
Lu	0.75	0.74	1.21	0.56	1.86	0.264	0.86
Hf	11.4	12.3	25.0	13.2	20.0	10.1	12.4
Ta	0.173	1.26	0.259	0.84	1.15	0.305	0.54
Pb	4.34	10.9	17.0	6.2	22.1	20.4	12.5
Th	5.7	11.6	10.0	3.63	11.2	18.2	8.3
U	1.54	5.0	1.93	1.90	2.75	1.91	1.91

Note: Oxides are weight percent, elements are parts per million. LOI—loss on ignition.

TABLE 3. MAJOR AND TRACE ELEMENT DATA FOR ROCKPORT GRANITE SAMPLES, ADIRONDACK LOWLANDS, NEW YORK STATE, USA

	JC7	JC16	JC19	JC21	JC22	JC48	JC49	JC50	JC51	JC52	JC56	JC61	JC62
Lat (°N)	44.3124	44.3082	44.4646	44.4039	44.3345	44.4614	44.4614	44.4614	44.4614	44.3666	44.3840	44.4189	44.3197
Long (°W)	75.9818	75.9840	75.7583	75.7975	75.9069	75.7109	75.7109	75.7109	75.7109	75.7619	75.9391	75.9745	75.9299
SiO_2	74.93	76.01	75.02	73.29	75.08	71.6		75.58		69.78	71.99	73.09	76.38
Al_2O_3	13.90	13.92	13.78	13.49	14.36	15.47		13.8		14.6	14.61	14.92	12.80
Fe_2O_3	1.96	0.98	1.64	3.05	0.98	1.74		1.31		2.94	1.96	1.42	1.74
MgO	0.20	0.10	0.30	0.20	0.20	0.10		0.10		0.90	0.70	0.40	0.40
CaO	0.89	0.69	0.67	1.22	0.84	0.92		0.83		2.84	0.94	1.45	0.72
Na_2O	3.75	4.55	3.23	3.84	4.44	6.41		5.33		4.60	4.25	4.32	2.86
K_2O	5.13	4.54	5.69	5.49	4.89	3.80		3.57		3.80	5.02	4.37	4.89
TiO_2	0.17	0.10	0.22	0.25	0.12	0.36		0.07		0.35	0.33	0.19	0.28
P_2O_5	<0.01	0.02	0.05	0.04	0.04	0.07		0.01		0.11	0.09	0.07	0.04
MnO	0.01	0.01	<0.01	0.03	0.01	0.01		0.02		0.04	0.02	0.01	0.01
LOI	0.58	0.39	0.68	0.95	0.64	0.43	2.08	0.52	0.55	0.62	0.82	0.74	1.34
Total	101.52	101.31	101.28	101.85	101.6	100.91		101.14		100.58	100.73	100.98	101.46
Li	10.2	11.2	9.7	15.8	16.1	3.15	2.64	8.1	5.7	9.2	28.5	5.0	32.1
Be	2.93	3.16	1.81	2.48	4.31	4.27	4.28	3.30	4.75	2.27	2.98	1.28	3.48
Sc	2.77	1.49	3.28	2.21	2.25	1.92	3.1	4.08	2.49	4.03	3.37	3.34	2.87
V	6.7	4.44	9.2	3.32	4.83	1.25	1.92	2.53	0.82	17.5	9.4	11.5	8.6
Cr	0.45	0.38	0.69	0.38	0.96	0.18	0.16	0.25	0.25	2.6	0.61	0.45	0.31
Co	1.03	1.21	1.63	2.09	0.78	1.04	0.91	1.12	0.93	3.54	2.22	1.08	2.46
Ni	0.48	0.93	0.98	0.58	0.46	0.29	0.33	0.34	1.04	1.72	0.61	1.44	0.71
Cu	<0.05	2.8	0.35	1.4	0.79	0.13	0.33	<0.05	1.6	0.73	6.9	0.45	0.15
Zn	4.1	8.9	6.3	40	8.2	12.7	20.2	28	23.4	12.2	45	2.8	10.3
Ga	22.1	21.2	19.8	23.8	21.5	23.2	23.7	22.8	21.8	22.2	22.2	19.6	21.2
Rb	186	182	160	169	195	114	87	149	113	60	167	28.6	168
Sr	108	84	105	93	136	61	55	70	84	301	359	329	332
Y	18.7	45.5	35.2	45.1	37.6	55	47.0	43.8	38.6	37.3	18.5	9.9	12.0
Zr	190	105	239	446	134	60	84	71	105	202	225	282	148
Nb	11.2	14.6	9.8	18.4	14.5	15.4	13.3	18.0	10.8	13.0	11.9	7.1	12.4
Mo	0.56	0.11	0.13	0.63	0.35	0.04	0.04	0.05	0.06	0.16	2.2	0.18	0.13
Sn	1.10	3.4	2.5	1.97	3.7	4.3	3.5	4.8	3.0	2.40	2.6	2.6	2.06
Cs	1.10	1.25	0.99	0.454	1.99	0.218	0.293	0.333	0.213	0.220	2.80	0.74	2.33
Ba	456	279	566	260	552	164	111	168	226	558	755	292	945
La	45.4	38.5	60	106	40.5	14.2	8.71	12.0	10.7	23.3	40.4	23.2	21.3
Ce	92	78	129	185	82	29.6	19.7	27.4	23.4	63	81	68	41.1
Pr	10.5	8.9	15.1	19.8	8.4	3.70	2.71	3.75	3.09	9.1	8.9	9.4	4.55
Nd	37.5	32.4	56.3	65.2	29.0	15.1	11.6	15.9	12.9	38.7	31.4	34.9	15.9
Sm	6.5	7.3	11.0	10.4	5.3	4.85	3.69	4.50	3.61	8.8	5.2	5.4	2.88
Eu	0.69	0.57	1.00	1.16	0.67	0.429	0.369	0.53	0.478	1.38	0.86	0.85	0.59
Gd	4.78	7.0	8.6	8.4	4.75	6.0	4.54	4.51	3.92	7.5	3.92	3.23	2.19
Tb	0.63	1.26	1.16	1.27	0.82	1.24	0.95	0.82	0.75	1.17	0.54	0.389	0.320
Dy	3.28	7.9	6.3	7.6	5.4	8.7	6.7	5.5	5.2	7.0	3.14	1.98	1.88
Ho	0.62	1.57	1.21	1.56	1.18	1.87	1.54	1.27	1.20	1.35	0.64	0.366	0.371
Er	1.74	4.40	3.30	4.39	3.68	5.5	4.81	4.28	3.88	3.65	1.87	1.00	1.08
Tm	0.276	0.67	0.476	0.67	0.61	0.87	0.81	0.79	0.67	0.55	0.307	0.165	0.179
Yb	1.92	4.12	3.00	4.36	4.16	5.4	5.7	5.9	4.79	3.48	2.16	1.20	1.29
Lu	0.310	0.56	0.471	0.67	0.67	0.73	0.90	1.00	0.79	0.54	0.356	0.189	0.211
Hf	6.5	3.81	7.7	12.9	4.70	2.32	3.78	2.93	4.05	5.4	6.7	7.5	4.51
Ta	0.371	2.11	0.472	0.73	1.54	2.44	2.30	2.32	1.77	1.24	0.78	0.399	1.72
Pb	5.9	7.7	9.2	8.5	11.4	18.2	17.9	19.0	27.6	7.4	10.6	1.50	10.2
Th	23.1	19.1	25.8	13.8	18.1	6.4	9.9	11.4	8.1	2.41	16.5	5.6	13.2
U	4.96	4.67	3.70	3.11	13.6	6.9	7.8	10.2	14.1	1.03	5.7	1.63	6.2

Note: Oxides are weight percent, elements are parts per million. LOI—loss on ignition.

TABLE 4. MAJOR AND TRACE ELEMENT DATA FOR CROW LAKE PLUTON SAMPLES, FRONTENAC SUITE, ONTARIO, CANADA

	DH1	DH2	EHW01	EHW02	JJF1	JK01	JK02	JT1	JT2	KC01	LJT1	MEW1	MEW2	MP1	MP2
Lat (°N)	44.5374	44.5427	44.5581	44.5581	44.5127	44.5123	44.5135	44.5353	44.5353	44.5581	Sand Lake	44.5123	44.5135	44.5353	44.5353
Long (°W)	76.2630	76.2646	76.2739	76.2739	76.2920	76.2918	76.2927	76.2794	76.2792	76.2739	area	76.2918	76.2927	76.2794	76.2794
SiO_2	72.08	70.7	71.02	67.68	47.04	51.96	47.83	68.07	48.75	67.94	69.15	43.47	48.73	68.32	50.72
Al_2O_3	14.40	15.14	14.67	16	14.30	15.70	15.33	14.80	15.12	15.75	14.06	13.69	15.44	14.66	15.63
Fe_2O_3	3.58	3.68	3.94	4.75	14.84	10.17	10.04	5.23	12.9	4.38	3.8	13.85	11.87	4.92	11.26
MgO	0.82	0.94	1.08	1.44	5.71	4.98	4.13	1.57	4.38	1.40	0.83	6.27	5.13	1.36	3.81
CaO	1.40	1.03	1.19	1.33	3.96	3.96	7.51	0.91	5.77	1.37	1.48	5.20	4.87	0.83	5.23
Na_2O	3.26	3.17	2.86	3.32	3.5	3.49	3.52	2.65	3.91	3.43	3.01	1.89	3.45	2.74	3.80
K_2O	5.83	6.46	6.13	6.03	4.38	4.52	4.12	6.76	3.76	6.08	5.80	6.40	4.39	6.70	4.46
TiO_2	0.16	0.23	0.24	0.28	2.57	1.65	2.18	0.31	1.94	0.32	0.21	3.12	1.88	0.28	1.71
P_2O_5	0.82	0.94	1.08	1.44	5.71	4.98	4.13	1.57	4.38	1.4	0.83	6.27	5.13	1.36	3.81
MnO	0.02	0.01	0.02	0.02	0.05	0.03	0.05	0.02	0.22	0.03	0.02	0.05	0.04	0.02	0.06
LOI	1.07	1.23	0.83	0.83	1.26	1.97	2.95	1.18	0.24	0.81	0.99	2.68	1.66	0.00	1.30
Total	103.44	103.53	103.06	103.12	103.32	103.41	101.79	103.07	101.37	102.91	100.18	102.89	102.59	101.19	101.79
Sc	3.87	2.00	5.34	4.92	9.86	12.1	13.1	4.77	11.8	5.15	6.93	10.8	11.8	4.21	11.4
V	28.8	42.7	50.7	46.9	241	141	187	45.0	202	41.7	40.9	244	178	38.8	171
Cr	2.95	4.92	7.30	7.52	2.21	12.5	2.31	0.00	4.12	5.97	3.44	6.15	2.56	0.00	1.75
Co	61.3	67.7	60.0	55.9	46.8	31.4	38.0	40.3	47.3	36.1	42.2	48.0	45.2	53.7	37.0
Ni	4.55	5.33	8.28	6.82	10.9	11.8	8.92	2.85	11.5	7.36	4.56	10.7	6.45	2.46	7.94
Cu	1.20	1.16	14.4	6.87	0.00	7.88	4.10	0.00	9.31	3.94	1.50	3.55	7.27	0.00	7.06
Zn	36.1	36.7	38.9	57.1	121	60.2	77.1	41.7	113	65.1	27.6	82.6	89.6	38.1	86.5
Rb	127	153	116	126	198	75.6	75.5	135	73.3	150	138	100	122	137	96.0
Sr	235	412	599	366	510	1024	1575	464	1661	359	285	505	1772	436	1449
Y	32.8	32.3	58.2	73.9	65.7	51.2	62.4	52.9	52.8	75.7	70.4	59.3	48.0	60.1	55.3
Zr	178				40.9	21.2	32.5	554	77.2		262	49.3	66.2	512	104
Nb	17.2				22.1	16.6	17.1	34.0	16.5		30.2	17.1	16.1	35.5	18.5
Ba	463	795	931	1035	816	1482	1475	1064	1262	819	646	1254	2038	975	1367
La	35.0	36.7	54.0	59.9	119	74.9	85.7	84.8	75.7	83.0	66.3	91.6	73.9	103	78.2
Ce	77.9	86.5	135	168	242	165	187	209	167	204	164	205	163	255	172
Pr	11.0	13.2	21.6	27.4	33.5	24.8	28.4	31.2	25.5	30.8	24.3	31.1	24.3	38.1	26.0
Nd	38.6	48.1	78.5	96.6	115	91.0	106	105	94.6	105	84.2	114	87.9	126	95.5
Sm	7.46	8.86	15.2	18.4	19.8	16.6	19.6	18.2	17.5	19.6	15.7	20.4	15.7	21.4	17.5
Eu	1.56	2.07	2.56	3.05	3.30	3.84	4.55	3.20	3.88	3.24	2.42	4.16	3.65	3.50	3.85
Gd	5.51	6.48	10.9	12.8	13.6	11.7	13.9	11.7	12.1	13.7	11.2	13.8	10.8	13.7	12.3
Tb	0.93	1.02	1.81	2.20	2.03	1.72	2.05	1.87	1.81	2.34	1.97	2.01	1.56	2.20	1.84
Dy	5.33	5.90	9.90	12.3	10.4	8.90	10.5	9.86	9.28	13.0	11.4	10.0	7.93	11.5	9.45
Ho	1.12	1.17	2.05	2.56	2.11	1.76	2.04	1.95	1.83	2.66	2.48	1.96	1.56	2.32	1.88
Er	3.20	3.22	5.69	7.13	5.66	4.59	5.19	5.38	4.75	7.38	7.21	5.05	4.03	6.27	4.90
Tm	0.47	0.42	0.77	1.05	0.73	0.60	0.66	0.78	0.62	1.02	1.03	0.65	0.53	0.88	0.64
Yb	3.03	2.37	5.02	6.69	4.64	3.66	3.99	5.24	3.83	6.82	6.85	4.10	3.21	5.65	3.96
Lu	0.43	0.31	0.68	0.92	0.67	0.52	0.56	0.73	0.55	0.95	0.94	0.58	0.46	0.80	0.58
Hf	4.36				0.99	0.61	0.82	13.19	1.70		6.28	1.05	1.78	12.09	2.26
Ta	1.95				1.13	0.99	1.03	2.88	1.10		2.38	0.96	1.10	3.44	1.14
Pb	9.34	7.89	6.53	5.81	4.00	9.46	10.0	11.2	11.1	6.96	7.92	8.50	10.3	10.6	10.1
Th	5.14				5.32	2.71	3.06	7.27	3.26		7.00	5.67	5.15	9.95	3.01
U	1.52				1.85	0.67	0.93	2.15	0.83		2.14	1.84	2.17	2.22	1.14

Note: Oxides are weight percents, elements are parts per million. LOI—loss on ignition.

TABLE 5. MAJOR AND TRACE ELEMENT DATA FOR SOUTH LAKE PLUTON SAMPLES, FRONTENAC SUITE, ONTARIO, CANADA

	DH3	JJF2	JJF3	JK03	JT3	JT4	KC02	KC03	LJT2	LJT3	MEW3	MP3	MP4
Lat (°N)	44.4166	44.3731	44.3727	44.3727	44.4002	44.4002	44.3888	44.3888	44.4164	44.3985	44.3727	44.4002	44.4002
Long (°W)	76.1865	76.1990	76.1994	76.1994	76.2106	76.2106	76.2323	76.2323	76.1870	76.1862	76.1994	76.2106	76.2106
SiO_2	73.94	61.38	61.69	60.95	59.57	60.92	58.91	57.80	75.45	73.05	61.89	59.22	60.37
Al_2O_3	14.91	18.10	16.67	16.72	17.25	17.77	17.48	16.80	14.94	14.47	17.64	17.38	17.08
Fe_2O_3	1.65	5.37	5.92	6.21	5.65	5.67	6.87	7.29	1.31	1.82	5.55	6.50	4.72
MgO	0.42	1.20	1.18	1.25	1.19	1.50	1.64	1.41	0.01	0.55	1.03	1.27	1.22
CaO	0.90	3.58	3.34	3.46	3.74	3.27	3.86	4.01	0.97	0.55	3.31	3.73	3.81
Na_2O	3.81	4.32	4.17	4.74	4.40	4.76	4.55	4.24	4.52	3.86	4.37	4.52	4.10
K_2O	4.64	5.10	5.16	4.93	5.32	4.98	4.65	4.87	4.06	4.51	4.99	4.96	5.50
TiO_2	0.29	1.10	1.11	1.19	1.19	1.12	1.51	1.54	0.16	0.17	1.07	1.36	1.10
P_2O_5	0.08	0.45	0.46	0.47	0.46	0.45	0.80	0.68	0.03	0.06	0.44	0.53	0.43
MnO	0.00	0.06	0.10	0.12	0.09	0.09	0.09	0.11	0.00	0.00	0.09	0.09	0.05
LOI	1.20		0.64	0.84	0.49	0.57	0.65	0.57	0.53	0.96	0.63	0.69	1.66
Total	101.84	100.66	100.44	100.88	99.35	101.10	101.01	99.32	101.98	100.00	101.01	100.25	100.04
Sc	1.95	7.12	8.90	8.64	8.61	7.98	10.7	10.4	0.35	0	7.92	8.30	6.96
V	20.6	21.6	26.4	30.7	32.2	30.5	35.0	39.1	9.18	11.5	19.0	35.1	30.0
Cr	0.14	0	0.82	0.84	0	0.60	0	0.05	0	0	0	0	0
Co	103	20.8	28.5	31.3	18.8	30.1	31.0	25.8	86.2	71.9	34.7	18.7	25.4
Ni	3.20	2.19	3.49	3.48	2.40	2.65	2.73	2.64	2.66	2.29	2.53	2.71	2.70
Cu	1.65	0	0.44	0.01	0	0	0	0	0	0	0	0	0
Zn	0	50.1	49.5	114	44.3	71.3	54.8	64.1	0	0	76.3	42.9	39.7
Rb	78.5	78.1	87.9	66.4	77.1	73.5	56.6	67.9	71.8	67.3	75.6	60.4	66.3
Sr	304	668	526	485	643	556	597	621	943	463	638	467	448
Y	11.9	54.2	63.7	55.8	62.2	61.0	83.4	75.8	7.09	7.66	62.4	58.2	49.9
Zr	207									236			
Nb	6.94									2.21			
Ba	979	1619	1632	1551	2069	1544	1675	1855	815	644	1634	1558	1600
La	20.2	49.6	58.7	55.1	53.4	51.3	66.2	61.0	11.9	8.41	47.7	45.3	46.7
Ce	28.6	107	124	94.7	114	110	138	134	22.7	15.4	110	91.7	74.9
Pr	4.59	16.2	18.5	17.6	17.1	16.6	22.8	20.9	2.21	1.27	16.3	15.2	14.4
Nd	15.0	61.5	70.4	66.4	64.7	62.8	88.9	80.7	8.85	5.55	63.3	59.5	55.5
Sm	2.77	12.9	14.8	13.7	13.7	13.4	19.5	17.4	1.86	1.24	13.9	13.1	11.9
Eu	0.80	4.05	4.44	4.06	4.27	4.09	4.95	4.51	0.58	0.43	4.37	3.86	3.60
Gd	2.29	10.1	11.6	10.7	11.1	10.8	15.6	13.8	1.95	1.44	11.0	10.7	9.71
Tb	0.33	1.69	1.97	1.78	1.88	1.84	2.66	2.36	0.22	0.19	1.90	1.82	1.62
Dy	2.15	9.52	10.9	10.0	10.5	10.4	14.7	12.9	1.30	1.33	10.7	10.3	9.10
Ho	0.48	1.98	2.28	2.06	2.21	2.17	3.07	2.72	0.24	0.29	2.24	2.15	1.92
Er	1.48	5.36	6.10	5.58	6.02	5.92	8.16	7.26	0.64	0.94	6.06	5.82	5.19
Tm	0.25	0.73	0.80	0.75	0.80	0.78	1.05	0.95	0.13	0.19	0.81	0.77	0.69
Yb	1.50	4.69	5.04	4.71	5.09	4.97	6.65	6.04	0.60	1.19	5.10	4.86	4.30
Lu	0.23	0.67	0.71	0.68	0.74	0.72	0.95	0.87	0.08	0.19	0.72	0.71	0.64
Hf	5.37									6.79			
Ta	1.30									0.93			
Pb	10.4	14.0	14.4	13.0	8.95	9.43	8.43	10.4	18.9	5.79	13.3	8.31	8.38
Th	5.25									1.11			
U	2.79									2.86			

Note: Oxides are weight percents, elements are parts per million. LOI—loss on ignition; blank—no analysis was made.

TABLE 6. MAJOR AND TRACE ELEMENT DATA FOR EDWARDSVILLE PLUTON SAMPLES, ADIRONDACK LOWLANDS, NEW YORK STATE, USA

	AGS-1	AGS-11	AGS-15	AGS-2	AGS-24	AGS-26	AGS-31	AGS-34	AGS-4	AGS-43	AGS-44	AGS-45	AGS-48	AGS-5	AGS-54	AGS-8	AGS-15	AGS-39	AGS-55
Lat (°N)	44.4874	44.4981	44.1609	44.4874	44.4829	44.4821	44.4832	44.4857	44.4882	44.5014	44.5015	44.5006	44.4996	44.4914	44.4872	44.4936	44.1609	44.2663	44.4008
Long (°W)	75.5816	75.5825	75.7412	75.5816	75.5643	75.5706	75.5754	75.5757	75.5812	75.5926	75.5909	75.5788	75.5803	75.5792	75.5553	75.5797	75.7412	75.7209	75.5216
SiO_2	53.41	61.68	63.13	50.34	52.46	49.73	48.68	61.64	52.96	57.33	60.38	62.6	63.57	48.57	52.52	47.84	63.13	70.08	61.78
Al_2O_3	17.33	17.54	16.51	16.67	15.17	15.33	15.73	16.13	16.23	17.36	17.49	17.66	17.49	14.94	16.27	14.35	16.51	14.10	17.76
Fe_2O_3	9.58	3.63	3.80	10.76	12.01	13.18	11.94	3.74	10.24	6.15	5.43	3.46	3.93	13.47	10.26	13.88	3.80	3.64	4.30
MgO	3.35	0.87	0.96	4.96	4.06	5.03	5.67	1.78	3.72	2.06	1.62	1.22	0.85	5.98	3.43	5.58	0.96	0.84	0.91
CaO	5.11	1.72	2.52	6.22	6.18	7.93	8.59	3.09	5.57	3.21	2.64	1.86	1.41	9.82	6.33	8.71	2.52	1.22	0.91
Na_2O	4.01	4.45	4.63	3.97	4.31	3.63	3.55	4.44	3.53	3.98	4.69	4.40	3.95	3.20	4.18	2.88	4.63	3.24	4.88
K_2O	4.24	7.71	6.03	2.74	2.15	1.97	1.12	6.28	3.89	5.42	4.55	7.25	8.02	0.75	3.24	1.51	6.03	6.03	8.02
TiO_2	1.66	0.73	0.76	1.72	1.87	1.76	2.14	0.11	1.84	1.27	1.26	0.98	0.76	1.78	1.79	1.84	0.76	0.59	0.59
P_2O_5	0.65	0.18	0.28	0.73	0.57	0.42	0.97	0.28	0.81	0.64	0.50	0.18	0.20	0.50	0.67	0.48	0.28	0.17	0.15
MnO	0.10	0.02	0.04	0.10	0.17	0.17	0.17	0.05	0.13	0.03	0.03	0.02	0.04	0.17	0.15	0.14	0.04	0.03	0.06
LOI	0.51	0.73	1.96	nd	0.73	0.84	1.82	1.12	0.94	1.18	1.02	1.07	0.59	0.82	0.74	0.81	1.96	0.50	0.55
Total	99.95	99.26	100.62	98.21	99.68	99.99	100.38	98.66	99.86	98.63	99.61	100.70	100.81	100.00	99.58	98.02	100.62	100.44	99.91
Li		9.3		30.6					26.3				11.1		16.0				
Sc		9.3		23.7					18.2				13.3		20.2				
V		35		217					159				38		157				
Cr		2		17					11.3				3		10				
Co		44.8		43.4					41.5				55.4		48.5				
Ni		1.8		20					10.33				1.9		13.2				
Cu		4.21		12.91					13.75				17.02		18.77				
Zn	61.4	17.4	31.9	65.8	92.5	105.5	104.2	16.6	64.9	41.4	41.8	18.4	34.3	80.8	89.2	88.4	31.9	23.0	44.2
Ga	21.7	19.9	18.5	24.7	19.1	18.0	18.6	16.9	22.2	20.2	22.0	17.5	18.6	17.9	21.4	17.9	18.5	15.0	18.9
Rb	69.8	31.3	119.6	61.1	64.6	44.1	14.2	58.8	47.0	72.8	81.0	83.8	38.7	5.8	42.4	27.0	120	111	186
Sr	661	111	345	799	393	537	653	186	834	522	346	135	208	607	636	604	345	262	612
Y	54.6	25.1	31.9	41.3	35.7	32.6	37.4	40.5	42.1	34.9	20.0	35.3	26.7	33.4	40.5	34.9	31.9	31.0	37.1
Zr	390		453		460	186	80	153		203	483	848		61		120	453	415	154
Nb	15.8		14.6		21.5	9.0	8.6	1.2		10.7	11.0	14.1		5.3		8.7	14.6	11.0	32.2
Mo		0.89		0.54					0.81				0.92		0.54				
Sn		1.8		2.4					2.3				2.2		2.7				
Cs		0.3		1					1				0.3		0.4				
Ba	1786	554	1384	1274	737	827	584	1588	2320	2918	1565	609	989	454	1796	916	1384	824	472
La		25.5		48.6					52.6				20.5		45				
Ce	137	59.79	155	128.8	113	66	108	69	142.1	115	104	85	51.08	61	121.5	65	155	188	146
Pr		7.4		14.3					16.1				6.8		14				
Nd		37.2		71.5					77.4				38.9		66.6				
Sm		7.1		11.5					12.7				7.3		11.4				
Eu		2.7		2.3					2.7				2.6		2.7				
Gd		6.5		10.2					10.9				7.3		10.1				
Tb		0.8		1.2					1.3				0.9		1.3				
Dy		5.6		8.8					9.1				6.1		8.7				
Ho		1		1.4					1.5				1.1		1.5				
Er		2.5		4					4.2				2.7		3.8				
Tm		0.4		0.5					0.6				0.4		0.5				
Yb		2.2		3.7					3.9				2.5		3.8				
Lu		0.3		0.5					0.5				0.3		0.5				
Pb		8.48		7.9					10.28				12.18		7.9				

Note: Oxides are weight percents, elements are parts per million. AGS-15—Diana Complex near Philadelphia (New York), AGS-39—Honey Hill pluton, AGS-55—Beaver Creek pluton. Blanks—no analysis was made.

TABLE 7. SENSITIVE HIGH-RESOLUTION ION MICROPROBE REVERSE GEOMETRY ANALYTICAL DATA FROM FRONTENAC SUITE SAMPLES IN THE ADIRONDACK LOWLANDS

Spot name	U (ppm)	Th/U	$^{204}Pb/^{206}Pb$	$^{207}Pb/^{206}Pb$	^{206}Pb (% com)	$^{206}Pb/^{238}U$	$^{206}Pb/^{238}U$ (error ±)	$^{207}Pb/^{206}Pb$	$^{207}Pb/^{206}Pb$ (error ±)	Disc. (%)
AGS45-1.1	117	0.55	–0.000058	.0803	–0.10	1138.2	8.1	1204	25	6
AGS45-10.1	61	0.70	0.000074	.0791	0.12	1165.9	11.8	1174	36	1
AGS45-2.1	154	1.07	–0.000075	.0801	–0.13	1132.2	7.0	1199	23	6
AGS45-3.1	110	0.37	0.000107	.0781	0.18	1149.0	8.4	1149	29	0
AGS45-4.1	57	1.08	0.000172	.0759	0.29	1162.3	11.4	1093	43	–6
AGS45-5.1	53	1.17	0.000209	.0768	0.35	1144.9	11.8	1116	51	–3
AGS45-6.1	49	0.61	–0.000120	.0808	–0.20	1156.0	12.7	1216	39	5
AGS45-7.1	43	0.73	–0.000049	.0806	–0.08	1137.7	13.5	1212	37	7
AGS45-8.1	63	0.98	0.000047	.0791	0.08	1166.8	11.4	1175	32	1
AGS45-8.2	105	0.39	–0.000117	.0820	–0.19	1152.6	9.0	1246	30	8
AGS45-9.1	27	0.74	–0.000217	.0812	–0.36	1162.3	17.4	1227	58	6
AGS45-9.2	80	0.43	0.000000	.0789	0.00	1156.4	9.9	1169	27	1
AGS49-1.1	75	1.04	0.000044	.0793	0.07	1106.2	10.5	1181	31	7
AGS49-2.1	40	0.58	0.000144	.0788	0.24	1152.8	14.6	1166	47	1
AGS49-4.1	68	1.00	0.000204	.0773	0.34	1179.8	9.2	1129	44	–4
AGS49-5.1	112	0.94	0.000056	.0774	0.09	1130.5	7.1	1131	22	0
AGS49-6.1	61	0.74	0.000070	.0787	0.12	1149.1	9.5	1165	28	1
AGS49-7.1	95	0.80	0.000030	.0789	0.05	1132.8	9.0	1169	26	3
AGS49-8.1	75	0.80	0.000108	.0776	0.18	1161.6	10.5	1138	48	–2
AGS49-9.1	89	0.98	0.000071	.0770	0.12	1156.1	9.5	1121	29	–3
AGS39-1.1	462	0.57	0.000022	.0785	0.04	1163.5	3.6	1160	10	0
AGS39-2.1	294	0.64	0.000000	.0790	0.00	1168.9	4.9	1173	13	0
AGS39-3.1	54	0.63	0.000104	.0773	0.18	1157.2	11.7	1130	40	–2
AGS39-4.1	1449	0.76	0.000006	.0738	0.01	649.6	22.4	1037	36	60
AGS39-5.1	241	0.56	0.000013	.0788	0.02	1141.7	5.6	1166	16	2
AGS39-6.1	153	0.58	0.000094	.0774	0.16	1182.8	8.3	1132	25	–4

Note: Uncertainties reported at 1σ. Spot notation: e.g., AGS45-8.2: AGS45—sample number, 8—crystal number, 2—spot on that crystal. See text for analytical details. Disc. —discordance; com—common.

and Nd anomalies relative to primitive mantle) indicating a suprasubduction zone origin (Chiarenzelli et al., 2010b). In addition, linear belts of gabbroic and amphibolitic rocks and mafic members of the Antwerp-Rossie suite have nearly identical geochemical trends. This suggests a widespread metasomatic enrichment during subduction of the upper mantle wedge that was the source for magmatic rocks in the Adirondack Lowlands. This source seems to have been absent soon after the Shawingan orogeny, because subsequent magmatic rocks lack the characteristic geochemical trends linking the Pyrites complex and associated plutonic rocks, and indicate the influence of a deeper enriched asthenospheric source for anorthositic and gabbroic members of the AMCG suite (Regan et al., 2011).

TABLE 8. LASER FLUORINATION OXYGEN ISOTOPE DATA FROM FRONTENAC SUITE ZIRCONS, ADIRONDACK LOWLANDS

Sample name	Weight (mg)	CO_2 (μmol)	$\delta^{18}O$ (‰ SMOW)
AGS-15	1.0	11.0	8.36
AGS-15	1.0	10.3	7.58
AGS-39	1.3	13.0	9.85
AGS-45	2.3	16.4	11.15
AGS-49	2.0	20.2	9.02
AGS-49	2.0	20.2	9.09

Note: Uncertainties on standards are typically <0.1‰ (1σ). Poor replication of AGS-15 may indicate a heterogeneous zircon population or inheritance. SMOW—standard mean ocean water.

1182 Ma Hermon Granitic Gneiss

The Hermon suite of hornblende granitic gneisses, often containing distinctive K-feldspar augen and megacrysts, is also found southeast of the BLSZ. The Hermon granite is slightly younger than the Antwerp-Rossie suite, 1182 ± 7 Ma (U-Pb zircon by SHRIMP II; Heumann et al., 2006). The Hermon granite is metaluminous, magnesian, and progresses from alkalic to alkali-calcic to calc-alkalic with increasing silica. Samples of Hermon granite plot mostly within the volcanic arc field of granites (Figs. 4E, 4F; see also Carl and deLorraine, 1997). Individual Hermon granite bodies tend to be compositionally homogeneous, but they range in SiO_2 from 54% to 75% (Carl and deLorraine, 1997). The Hermon granite has several geochemical similarities to the felsic members of the Antwerp-Rossie suite, although it is somewhat more potassic (Fig. 4D). The Hermon suite has similar to slightly higher LREE enrichment (La_n/Sm_n = 2.4–6.5; av. = 3.9) and moderately depleted HREEs (Sm_n/Yb_n = 1.6–9.3, av. = 4.9) compared to the Antwerp-Rossie suite. The Hermon granite also shares the high Cs, La, and Nd, and low Nb, P, and Ti, and a similar Nd isotope composition with the Antwerp-Rossie suite (Fig. 4H) (Chiarenzelli et al., 2010b).

However, there are several geochemical differences between the two suites. The Hermon granite is more potassic (K_2O 4.7% ± 1.0%) than the Antwerp-Rossie suite (K_2O 3.8% ± 0.7%), and more felsic (SiO_2 65% ± 5% compared to 63% ± 8%), has higher Ta (5.6 ± 3.9 ppm compared to 1.7 ± 1.6 ppm) and Zr (>300 ppm at intermediate SiO_2 contents compared to 100–300 ppm), and lower Pb (2.3 ± 0.9 ppm compared to 17.6 ± 11.1 ppm). The tectonic setting of the Hermon granite is also somewhat ambiguous. Many of the geochemical characteristics described here are similar to those of the Antwerp-Rossie suite, and are consistent with subduction and genesis in a volcanic arc system. However, by 1182 Ma the Adirondack Lowlands was already undergoing thickening and metamorphism caused by collision with the Adirondack Highlands to the east, indicating that subduction might have already ceased (Heumann et al., 2006; Fig. 3). It is possible that the geochemical features of the Hermon granite reflect a subduction-related geochemical

signature in the metasomatized mantle that persisted after subduction had ceased (e.g., Pearce et al., 1990; Coulon et al., 2002; Till et al., 2009), or simply the lag time for the ascent of subduction-related melts.

A possible analog occurs in the Miocene Sonoran arc (Mexico) where calc-alkaline volcanic rocks continued to be erupted after subduction of the Farallon plate ended. This transition from subduction-related to postsubduction volcanism was marked by differences in trace elements that reflect changes in the source region (e.g., lower Nb/Ta), less slab-derived fluid contribution (e.g., lower Ba/Y), and smaller LREE/HREE in postsubduction lavas (Till et al., 2009). Similar characteristic differences are observed between the Antwerp-Rossie suite and Hermon granite: the Nb/Ta ratio changes from 9.4 ± 4.9 to 3.7 ± 2.0 and the Ba/Y changes from 56 ± 26 to 33 ± 13 (calculated using our new data and data from Chiarenzelli et al., 2010b). Generally, the REEs are less fractionated in the Hermon granite (La_n/Sm_n and Sm_n/Yb_n are lower) than in the Antwerp-Rossie suite. However, this reflects the general lack of strongly fractionated members of the Hermon granite ($La_n/Sm_n > 5$ and $Sm_n/Yb_n > 8$) compared to the Antwerp-Rossie suite, a feature similar to Miocene volcanic rocks in Sonora (Till et al., 2009). The geochronological constraints and the geochemical characteristics of the Hermon granite are consistent either with the end of Shawinigan subduction or, alternatively, derivation from a mantle source modified by subduction-related fluids shortly after subduction ended. The latter was perhaps caused by slab break-off or postcollisional extension following juxtaposition of the Frontenac terrane and Adirondack Lowlands.

It is interesting to note the differences in geographic locations of each of these suites. The Antwerp-Rossie suite primarily intrudes rocks of the "lower marble," to the north and west of Gouverneur, whereas the Hermon granitic gneiss primarily intrudes pelitic and pssamitic Popple Hill gneiss to the south and east of the Antwerp-Rossie suite (Fig. 2). This spatial distribution could be evidence of deflection or channeling of later melts into the relative weak and leucosome-rich Popple Hill gneiss as deformation and tectonism progressed.

1172 Ma Hyde School Granitic Gneiss

The Hyde School gneiss (hereafter HSG) occurs primarily in 14-km-scale structural domes within the Adirondack Lowlands from southeast boundary of the BLSZ southeast to the Carthage-Colton shear zone (Fig. 2). This distribution may suggest intrusion after the dominant structural architecture of the Adirondack Lowlands was established, in contrast to the more restricted occurrence of earlier suites. HSG bodies compose the most controversial

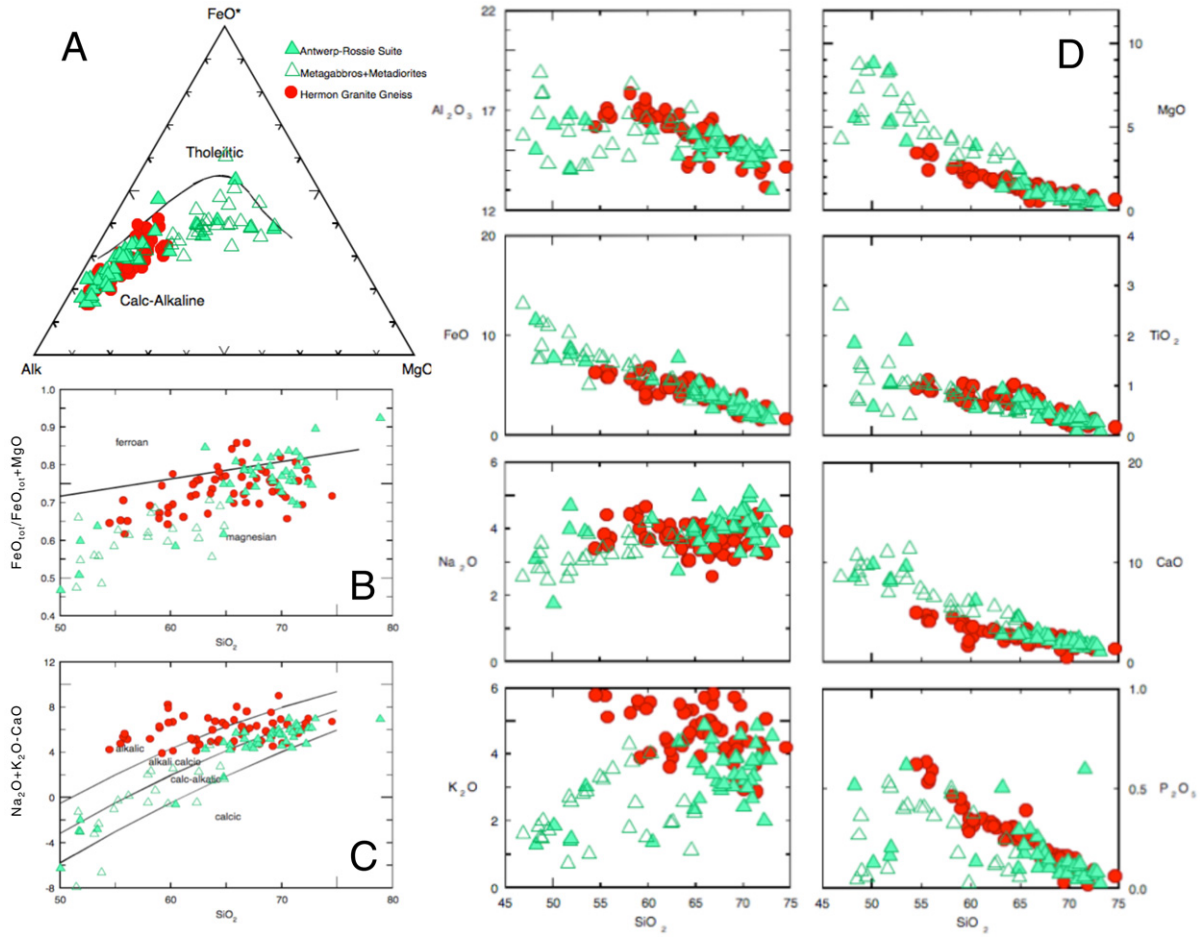

Figure 4. Geochemistry of the Antwerp-Rossie suite, correlative metadiorites and metagabbros, and Hermon granite (data from Carl and deLorraine, 1997; Carl, 2000; Chiarenzelli et al., 2010b; this study). (A) AFM ($Na_2O + K_2O$, FeO + Fe_2O_3, MgO) diagram; discriminant line after Irvine and Baragar (1971). (B, C) Classification diagrams of Frost and Frost (2008). (D) Major element–silica variation diagrams. (*Continued on following page*.)

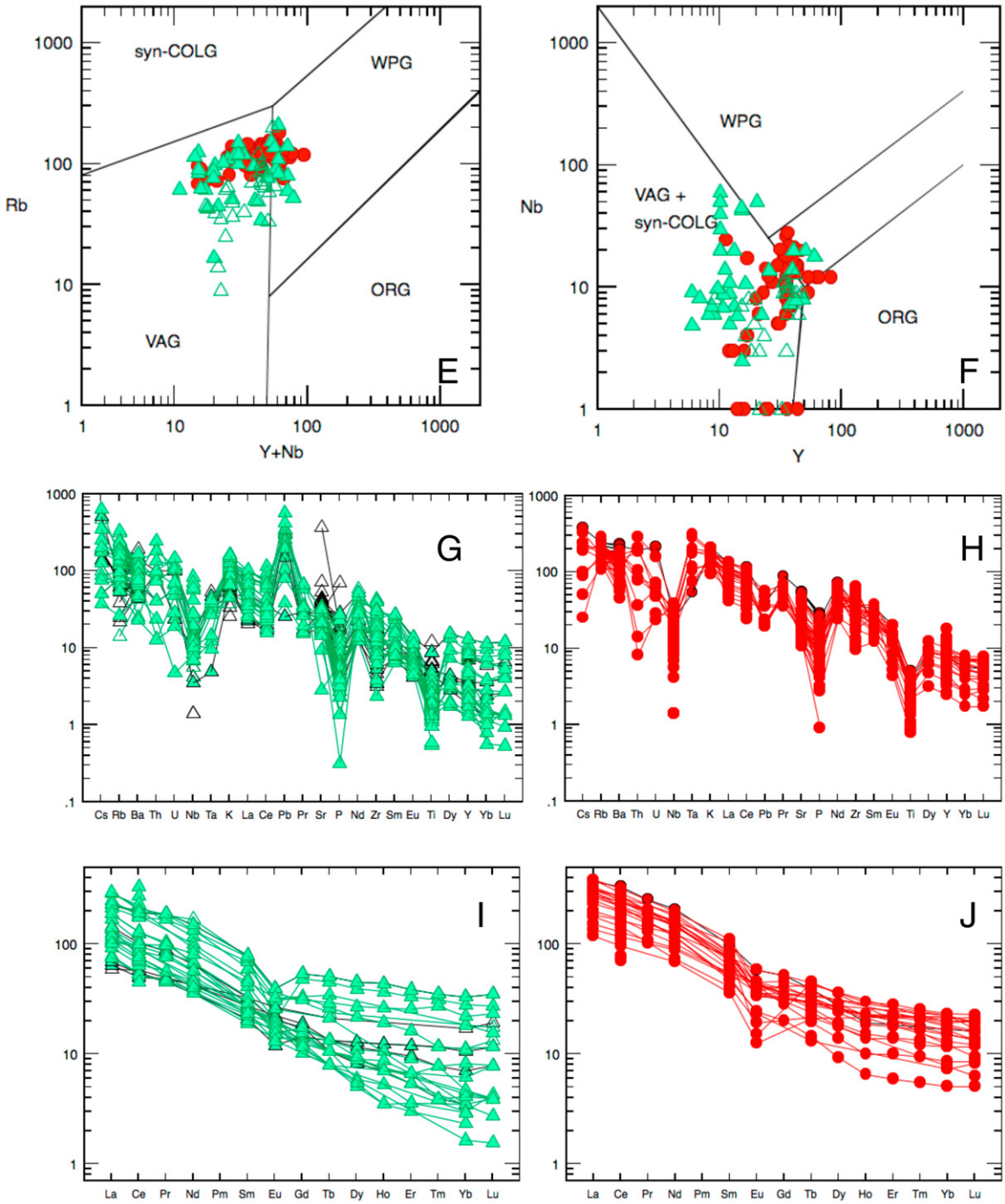

Figure 4 (*continued*). (E, F) Tectonic discrimination diagrams of Pearce et al. (1984). Syn-COLG—syn-collision granite, WPG—within-plate granite, VAG—volcanic arc granite, ORG—orogenic granites. (G, H) Multielement plots of the Antwerp-Rossie suite (G) and Hermon granite (H), normalized to primitive mantle (normalizing factors from Sun and McDonough, 1989). G excludes anomalously high Ta from Carl (2000). (I, J) Rare earth element plots of the Antwerp-Rossie suite (I) and Hermon granite (J) normalized to chondrite (Sun and McDonough, 1989). In G–J, rocks with <57% SiO_2 are shown with back symbol outlines and pattern lines.

igneous suite in the Adirondack Lowlands with respect to its origin. These domical bodies range from alaskite to tonalite in composition and contain both concordant amphibolite layers and amphibolite dikes that crosscut earlier layering.

Buddington (1929) interpreted the HSG to be plutonic bodies intruded as phacoliths, whereas Carl et al. (1990), Carl and deLorraine (1997), and Carl (2000) interpreted them as aerially extensive metamorphosed volcanic rocks forming the base of an Adirondack Lowlands supracrustal sequence. Geochemical zoning within these bodies was interpreted as relict of volcanic stratigraphy. The domical structure of the HSG bodies has been attributed to syntectonic intrusion, sheath folding, cross-folding, or as being the result of deformation during transpression (see Baird and Shrady, 2011).

McLelland et al. (1991) suggested that the HSG has a plutonic origin, and that rocks in contact with the HSG show contact-metamorphic temperatures higher than those of regional Shawinigan metamorphic isotherms (see also Hudson, 1994). Single-grain U-Pb dating of zircon from two bodies of HSG demonstrates that the HSG is contemporaneous with the 1172 Ma Rockport granite (Wasteneys et al., 1999). This age was also reported in one multigrain zircon population by McLelland et al. (1991), along with older inherited zircon. This 1172 Ma age is contemporaneous with garnet and monazite ages (Mezger et al., 1991), migmatite formation in the metapelitic rocks (Heumann et al., 2006), and penetrative deformation of the Adirondack Lowlands (Baird and Shrady, 2011). These relationships indicate that the current level of exposure was at depth at the time, supporting a plutonic origin for the HSG. Because Adirondack Lowlands metasediments are crosscut by the ca. 1203 Ma Antwerp-Rossie suite, the ca. 1172 Ma HSG, although apparently conformable with metasediments, must have intruded this package as well. Thus, the HSG cannot form the basement for the metasedimentary sequences of the Adirondack Lowlands (see also Peck et al., 2011).

The HSG ranges from intermediate to felsic (Fig. 5D), but typically has SiO_2 > 75% (McLelland et al., 1991), and straddles the metaluminous-peraluminous composition boundary (samples ≥75% SiO_2 have molar $Al_2O_3/(CaO + Na_2O + K_2O) \approx 0.9–1.2$). The felsic HSG is mainly ferroan, while rocks with <70% SiO_2 are magnesian. HSG samples define smooth trends on variation diagrams and straddle the alkali-calcic–calc-alkalic boundary (Figs. 5C, 5D). Conformable amphibolitic layers and crosscutting dikes in the HSG are geochemically similar and consistent with a comagmatic origin with the HSG (McLelland et al., 1991). The samples analyzed from the HSG plot transitionally between within-plate and volcanic arc granites, with the tonalitic facies making up the majority of samples in the volcanic arc fields (Figs. 5E,

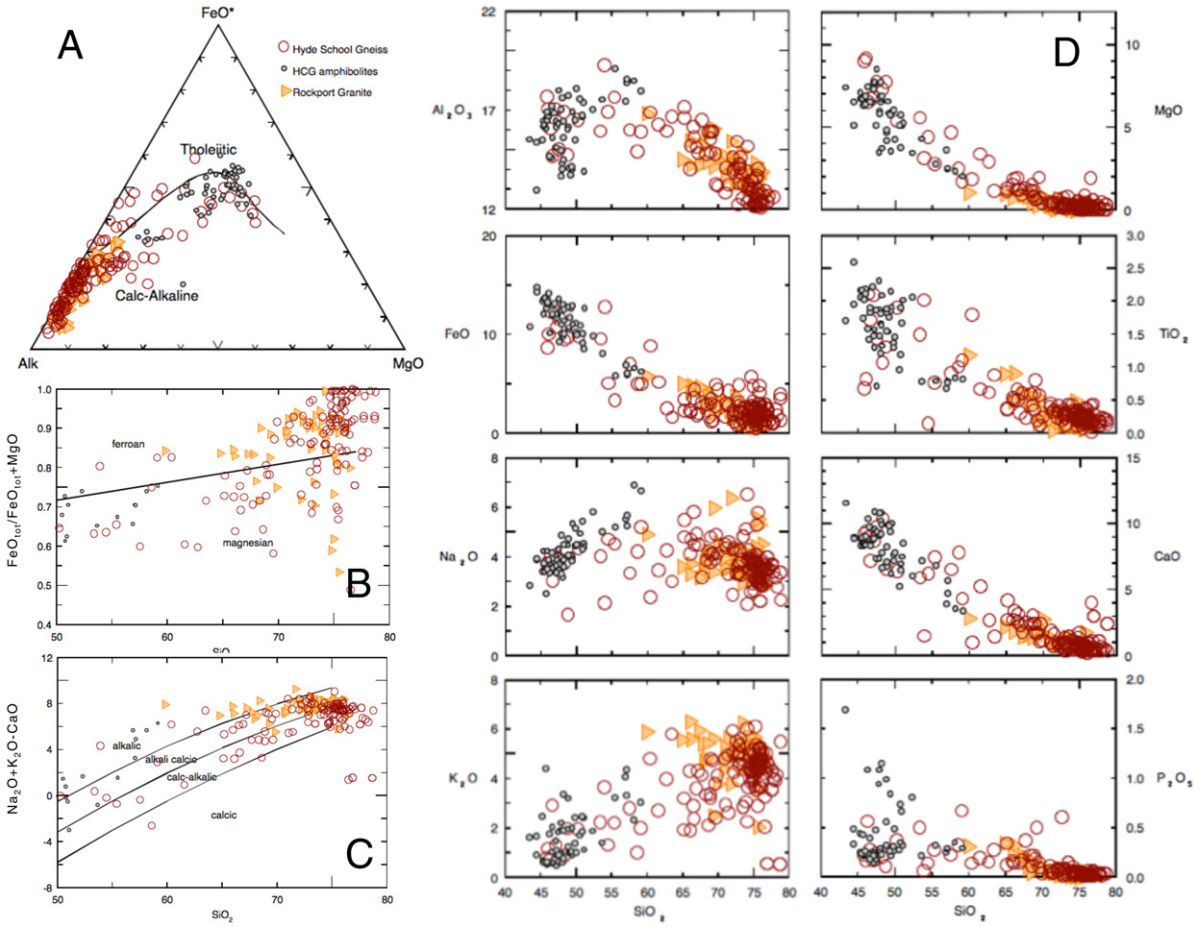

Figure 5. Geochemistry of the Hyde School gneiss (HSG), HSG amphibolite layers and dikes, and Rockport granite (data from Maher, 1981; Fischer, 1995; Carl and deLorraine, 1997; Carl, 2000; this study). (A) AFM ($Na_2O + K_2O$, $FeO + Fe_2O_3$, MgO) diagram after Irvine and Baragar (1971). (B, C) Classification diagrams of Frost and Frost (2008). (D) Major element–silica variation diagrams. (*Continued on following page*.)

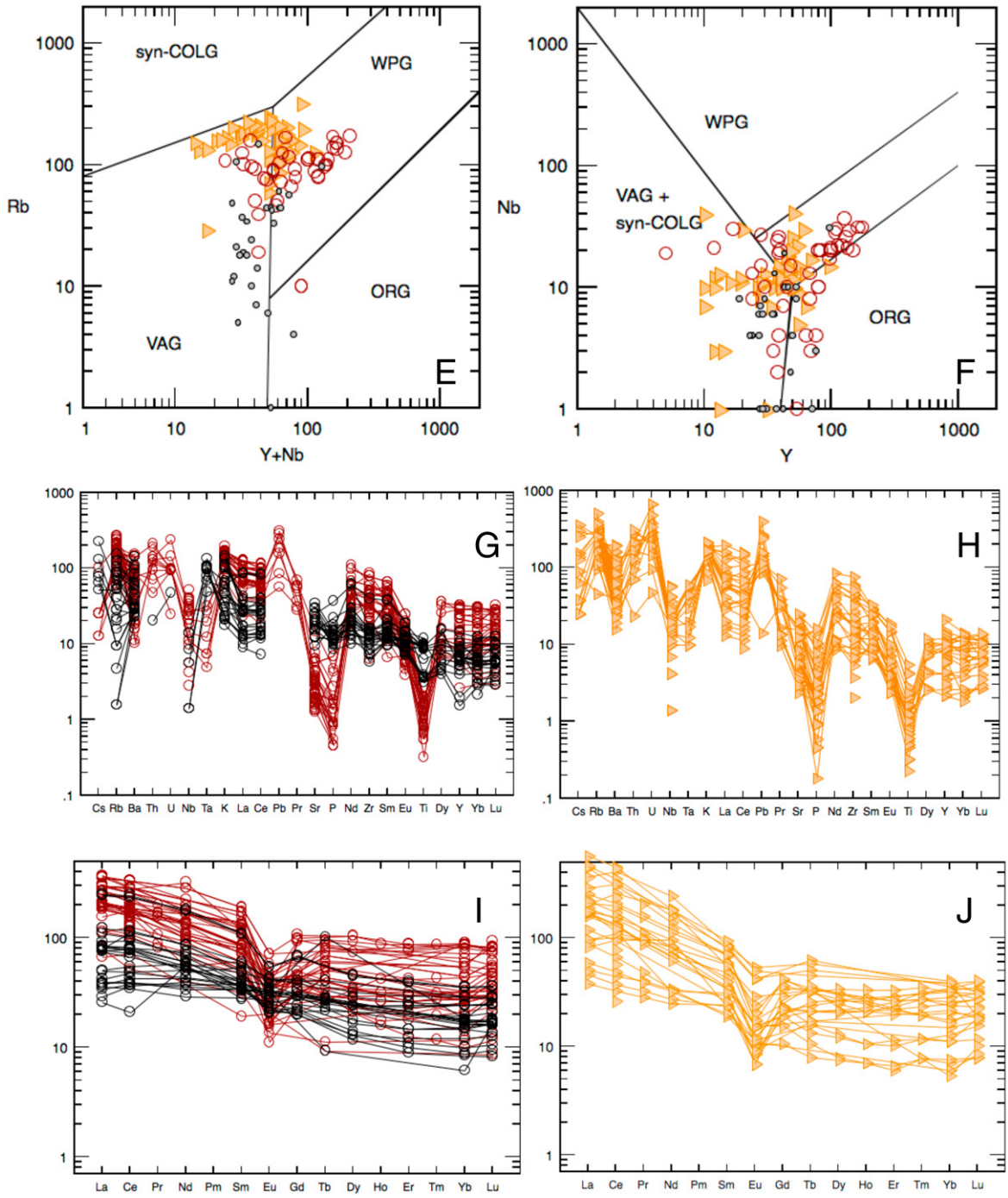

Figure 5 (*continued*). (E, F) Tectonic discrimination diagrams from Pearce et al. (1984). Syn-COLG—syn-collision granite, WPG—within-plate granite, VAG—volcanic arc granite, ORG—orogenic granites. (G, H) Multielement plots of the HSG (G) and Rockport granite (H) normalized to primitive mantle (Sun and McDonough, 1989). (I, J) Rare earth element plots of the HSG (I) and Rockport granite (J) normalized chondrite (Sun and McDonough, 1989). In G–J, rocks with <57% SiO_2 are shown with back outlines and pattern lines.

5F; Wasteneys et al., 1999). The HSG shows similar high Cs, Pb, La, and Nd, and low Nb, Ta, P, and Zr concentrations to the Antwerp-Rossie suite (Fig. 5G).

Overall, the HSG has high REE, moderate LREE enrichment (av. La_n/Sm_n = 2.5) and slightly depleted (relatively flat) HREE (av. Sm_n/Yb_n = 2.5), with moderate negative Eu anomalies (Fig. 5I). Tonalitic rocks of the HSG have slightly lower REEs and are more depleted in HREEs than more granitic lithologies (Sm_n/Yb_n > 2.5; McLelland et al., 1993). HREE patterns are consistent with a plagioclase-bearing, garnet-free parent rock, and concave-up HREE patterns indicate pyroxene or hornblende in the source. T_{DM} Nd ages for the HSG are characteristic of a depleted mantle, and range from 1.2 to 1.4 Ga (McLelland et al., 1993), similar to the Antwerp-Rossie suite and Hermon granite (Chiarenzelli et al., 2010b).

1172 Ma Rockport Granite

The Rockport granite is an igneous-textured to gneissic pink leucogranite that crops out on shores of the St. Lawrence River and islands therein, but does not extend southeast of the BLSZ. It is typically emplaced as dikes and sheets into metasedimentary country rocks, and in places forms spectacular net-vein textures where emplaced into calc-silicate gneiss (Carl and deLorraine, 1997). Deformed and recrystallized Rockport granite, massive igneous-textured Rockport granite, and isolated Rockport granite dikes all share ca. 1172 Ma crystallization ages (van Breemen and Davidson, 1988; Wasteneys et al., 1999). Single-grain U-Pb geochronology of Rockport granite on Wellesley Island (Wasteneys et al., 1999) showed that the age of 1416 ± 5 Ma previously determined by multigrain techniques (McLelland et al., 1991) was probably the result of xenocrystic zircon contamination and U-Pb discordance. In addition, texturally early gneissic Rockport granite is geochemically similar to rocks that crosscut it, indicating that the different phases of Rockport granite are comagmatic (Carl and deLorraine, 1997).

Wasteneys et al. (1999) interpreted the HSG and Rockport granite to be part of the same magmatic suite, based on lithologic similarities and U-Pb zircon ages. The HSG and the Rockport granite have similar SiO_2 (~71%–72%) and overlap on major element variation diagrams (Fig. 5D); their felsic facies are mostly ferroan, straddle the metaluminous-peraluminous boundary, and share similar positive Cs, Pb, La, and Nd, and negative Nb, Ta, P, and Zr anomalies (Figs. 5B, 5D, 5H). Plutonic bodies near North Hammond (New York State) are correlated with Rockport granite (Wong et al., 2011) because they share similar geochemical characteristics. The Rockport granite is weakly LREE enriched (av. La_n/Sm_n = 4.0) and has relatively flat HREE (av. Sm_n/Yb_n = 2.7), and moderate negative Eu anomalies. Most of these characteristics are similar to the HSG, but Rockport granite samples exhibit higher LREE enrichment and lower overall HREEs than HSG (Fig. 5J).

Similar to the HSG, HREE patterns of the Rockport granite are consistent with plagioclase-bearing and possibly pyroxene- or hornblende-bearing sources. A single Rockport granite sample has a Nd T_{DM} of 1.4 Ga, similar to the HSG (McLelland et al., 1993). The Rockport granite differs from the HSG in generally lacking associated tonalitic facies and amphibolite layers or dikes, higher average K_2O, and whole-rock chemistry that varies from alkali-calcic to calc-alkalic instead of largely calc-alkalic.

Most notable in the field is the difference in emplacement style of the two suites: HSG forms conformable domes within the enveloping metasedimentary rocks, whereas the Rockport granite intruded as crosscutting dikes and sheets into country rock. These distinct emplacement styles may be the result of differences in the stress field (e.g., Baird and Shrady, 2011) or country-rock lithologies on either side of the BLSZ. It is possible that the more ductile marble-rich country rocks of the Adirondack Lowlands southeast of the shear zone promoted concordant emplacement of the HSG (cf. Corriveau and Leblanc, 1995), while quartzite-rich country rocks of the Frontenac terrane northwest of the BLSZ promoted fracture-controlled emplacement of Rockport granite.

1150–1180 Ma Frontenac Plutonic Suite

A distinctive feature of the southwestern Grenville Province is the abundance of syn-Shawinigan to post-Shawinigan (i.e., 1.18–1.16 Ga) magmatism, including members of the AMCG suite. We focus here on suites that intruded the Adirondack Lowlands and Frontenac terranes, followed by a comparison with the contemporaneous magmatism in the nearby Adirondack Highlands, Central Metasedimentary Belt of Quebec, and Morin terrane (Fig. 1).

The Frontenac suite has been well described and dated in Ontario. It is made up of granite, monzonite, syenite, gabbro, and anorthosite plutons emplaced into metasediments during the period 1154–1176 Ma (Marcantonio et al., 1990; Davidson and van Breemen, 2000; Peck et al., 2004; Grammatikopoulos et al., 2007). These plutons preserve igneous textures and original contact relationships with country rocks, except where deformed within the Maberly shear zone in the western Frontenac terrane and eastern Sharbot Lake domain (Davidson and van Breemen, 2000). Undeformed Frontenac suite plutons have unusually high $\delta^{18}O$ values (Fig. 6), which are interpreted as indicating derivation from a hydrothermally altered ocean crust component in the basement of the Frontenac terrane (Peck et al., 2004). Some of the Frontenac plutons are made up of several bodies having different igneous compositions that are separated by country-rock screens, and some bodies have magma mingling textures (Davidson and van Breemen, 2000; Grammatikopoulos et al., 2007).

Although the Frontenac suite was emplaced, in part, during emplacement of the Rockport granite and HSG, the suites are geochemically distinct. The Frontenac suite is generally more mafic than the Rockport granite and has a more continuous range of compositions (Figs. 7A–7D). The Rockport granite and HSG (>70% SiO_2) are commonly strongly ferroan, and the Frontenac suite straddles the ferroan-magnesian compositional boundary (Fig. 7B). The Rockport granite is largely alkali-calcic to calc-alkalic, while the Frontenac suite rocks are alkaline, especially the mafic and intermediate facies (Fig. 7C). Plutons of the Frontenac suite display differences in major element geochemistry. For example, P_2O_5 and SiO_2 (<50% SiO_2) (Fig. 7D) show a negative correlation for mafic rocks of the Crow Lake pluton and a positive relation for the Leo Lake pluton. The Frontenac suite has a continuous range of major elements compositions, but individual plutons vary. For example, our new data show that the South Lake and Crow Lake plutons are bimodal, with ~10% gaps in SiO_2 between mafic and felsic lithologies (Fig. 7D), similar to the bimodal Leo Lake pluton (Grammatikopoulos et al., 2007).

The Frontenac suite and the Rockport granite plot similarly as transitional between within-plate and volcanic arc granites (Figs. 7E, 7F). The Frontenac suite lacks, or has much less prominent, negative anomalies in Sr, P, and Ti than the Rockport granite, and shows negative anomalies in Zr, Th, and U (Fig. 7G). It has overall high REEs (LREE ~150–500× chondrite), except for a mafic sample from the Leo Lake pluton and three felsic samples from South Lake pluton, which have LREE ~10–80× chondrite. All Frontenac suite samples have moderate LREE enrichment (av. La_n/Sm_n = 2.7) and HREE depletion (av. Sm_n/Yb_n = 3.4), with negligible Eu anomalies (Fig. 7H). The Frontenac suite shows increasing Zr with SiO_2 until ~60%, after which Zr declines, a typical relationship for some A-type granites (Whalen et al., 1987). In contrast, the HSG has steadily increasing Zr with SiO_2 with the highest Zr in the most evolved rocks (Figs. 7I, 7J). T_{DM} Nd model ages for the

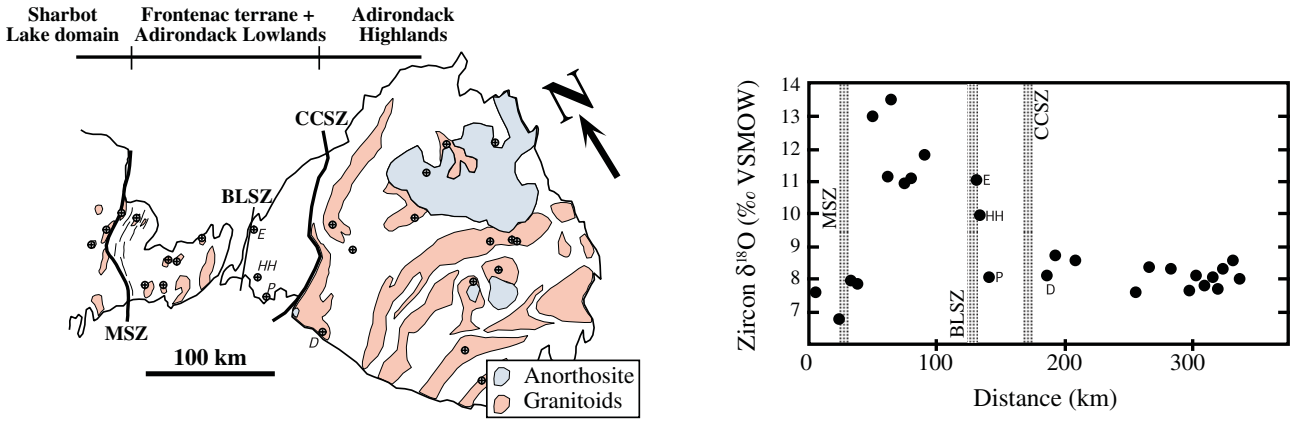

Figure 6. Oxygen isotope transect of the Frontenac suite and other AMCG (anorthosite-mangerite-charnockite-granite) related granitoids across the Adirondack Highlands, Frontenac terrane, and Sharbot Lake domain of the Elzevir terrane, showing $\delta^{18}O_{zircon}$ values as a function of distance perpendicular to terrane boundaries (after Peck et al., 2004). The high $\delta^{18}O_{zircon}$ values of the Frontenac terrane indicate the presence of high $\delta^{18}O$ rocks, possibly hydrothermally altered ocean crust and sediments, in the deep crust. E—Edwardsville, HH—Honey Hill, P—Philadelphia, D—Diana complex, MSZ—Maberly shear zone, BLSZ—Black Lake shear zone, CCSZ—Carthage-Colton shear zone, VSMOW—Vienna standard mean ocean water.

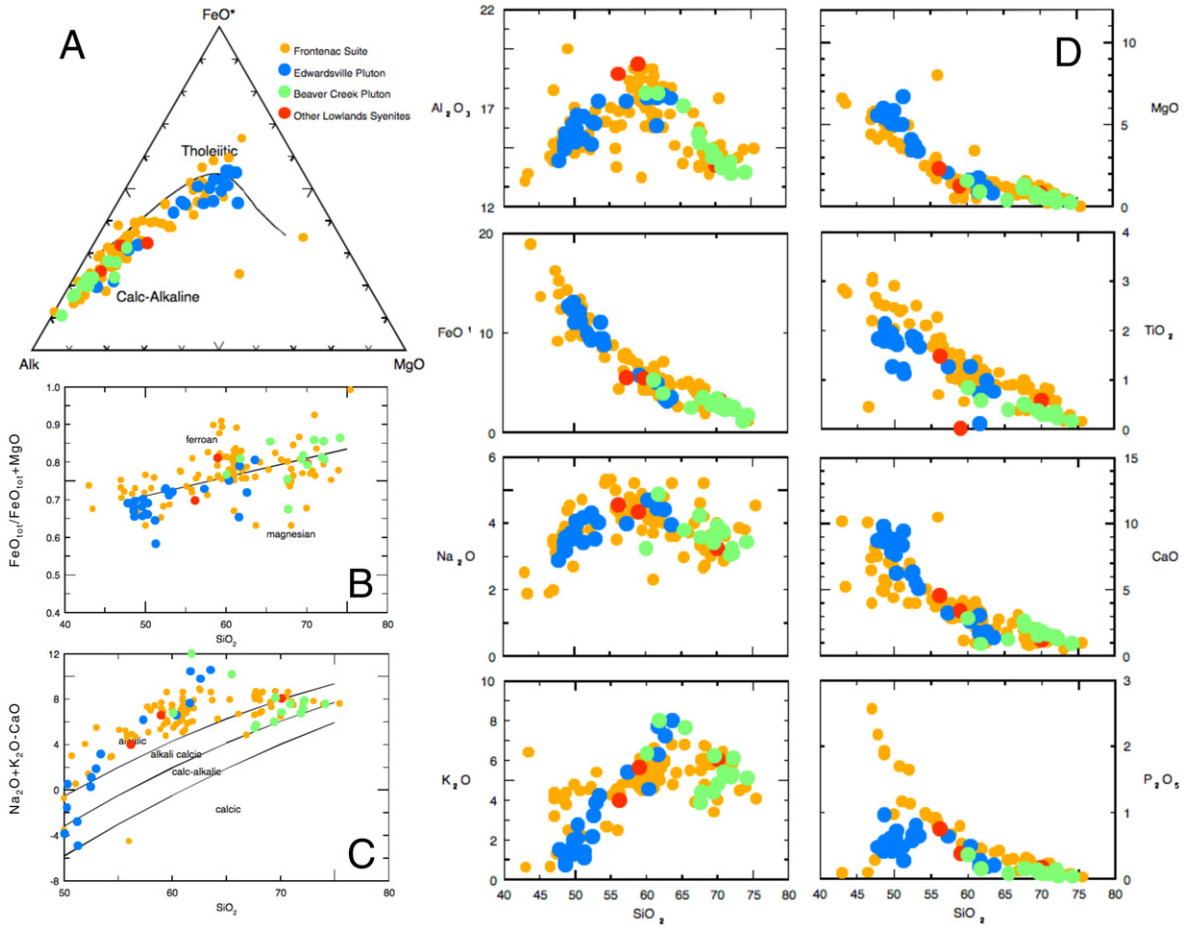

Figure 7. Geochemistry of the Frontenac suite, Edwardsville pluton, and other syenite plutons of the Adirondack Lowlands (data from Buddington, 1939; Ermanovics, 1970; Currie and Ermanovics, 1971; Marcantonio et al., 1990; Davidson, 1996; Carl and deLorraine, 1997; Carl, 2000; Grammatikopoulos et al., 2007; this study). (A) AFM (Na_2O + K_2O, FeO + Fe_2O_3, MgO) diagram after Irvine and Baragar (1971). (B, C) Classification diagrams of Frost and Frost, 2008. (D) Major element–silica variation diagrams. (*Continued on following page*.)

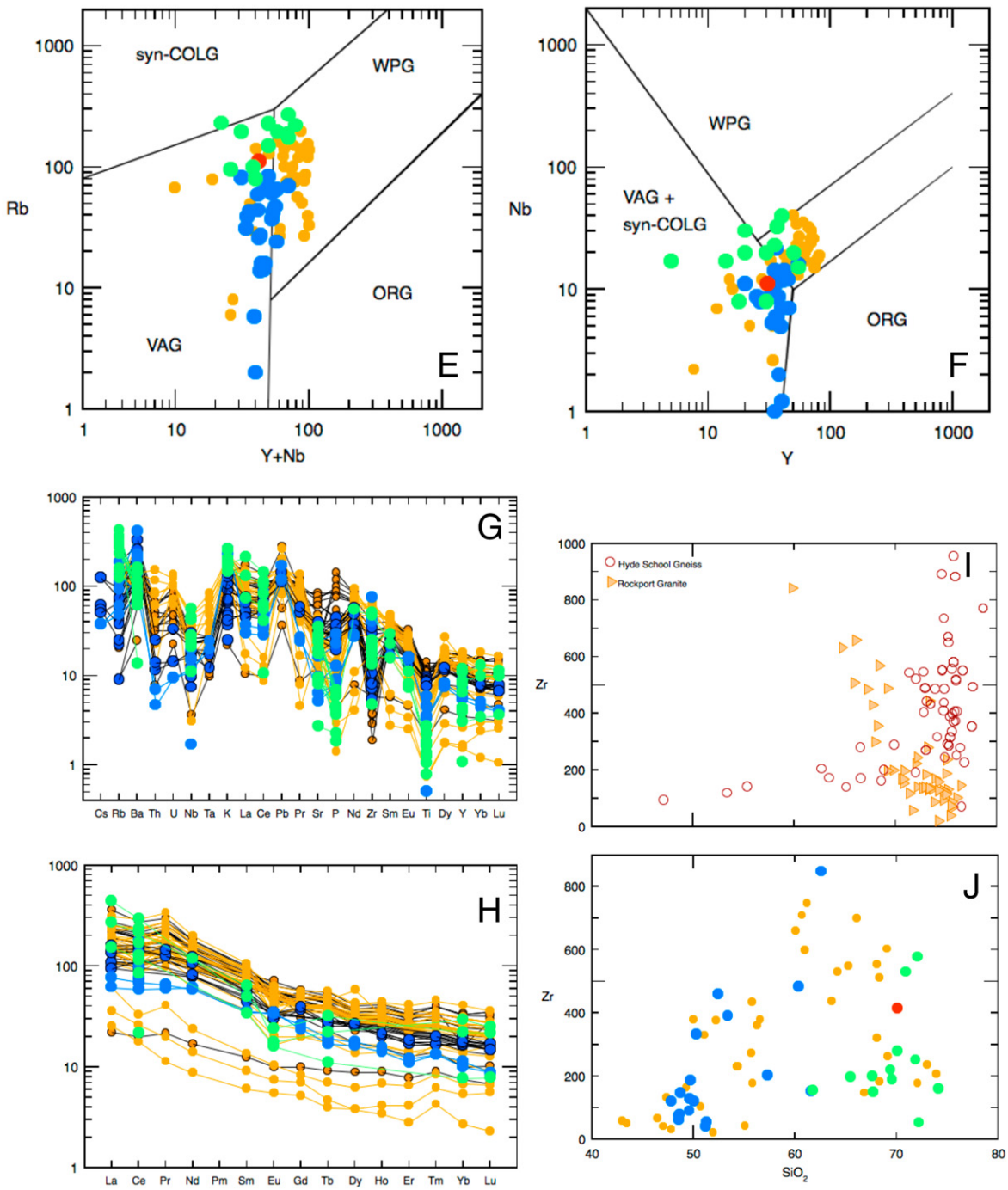

Figure 7 (*continued*). (E, F) Tectonic discrimination diagrams from Pearce et al. (1984). Syn-COLG—syncollision granite, WPG—within-plate granite, VAG—volcanic arc granite, ORG—orogenic granites. (G) Multielement patterns normalized to primitive mantle (Sun and McDonough, 1989), excluding anomalously high Ta (from Carl, 2000). (H) Rare earth element patterns normalized to chondrite (Sun and McDonough, 1989). (I, J) Hyde School gneiss and Rockport granite (I) and Frontenac suite and the Edwardsville pluton plots (J) of Zr versus SiO_2. Open circles are Hyde School gneiss and triangles are Rockport granite; other symbols as in A. In G and H, rocks with < 57% SiO_2 are shown with back outlines and pattern lines.

Frontenac suite range from 1.3 to 1.5 Ga (Marcantonio et al., 1990), similar to Antwerp-Rossie, Hermon granite, and Hyde School plutons.

Newly Recognized Frontenac Suite Plutons in the Adirondack Lowlands

Buddington (1934) described a number of syenite bodies in the Adirondack Lowlands that share lithologic characteristics and emplacement style with the Frontenac suite. McLelland et al. (1993) presented an isotope dilution–thermal ionization mass spectrometry (ID-TIMS) zircon date of 1164 ± 4 Ma from a felsic lithology of one of these bodies, the Edwardsville pluton. The Edwardsville pluton also shares the unusually high magmatic $\delta^{18}O$ of other members of the Frontenac suite, which led to a correlation of this body with this suite (Peck et al., 2004). Here we present new geochemistry and geochronology for the Edwardsville pluton and other syenite bodies in the Adirondack Lowlands that confirm their correlation with the Frontenac suite.

The Edwardsville pluton is a composite intrusive located immediately east of the BLSZ (Fig. 2). Parts of this body have been called the Pope Mills mass (Buddington, 1934), Edwardsville syenite (McLelland et al., 1993; Peck et al., 2004), and Pope Mills metagabbro (Carl, 2000). Buddington (1934, p. 69) mapped this pluton, and described it as "a belt of pink to red syenite…intrusive into a belt of pyroxenitic amphibolite with which it forms a migmatite"; he correlated the Pope Mills pluton with other mapped (but essentially unstudied) syenite bodies in the Adirondack Lowlands. The northern margin of the Edwardsville pluton is syenite containing occasional mafic enclaves and country-rock xenoliths. Mafic lithologies, making up the southern portion of the pluton, include fine-grained equigranular monzodiorite to diorite crosscut by melanocractic porphyritic monzonite (Fig. 8). Major element variation diagrams show smooth trends from fine-grained monzodiorite and diorite ($SiO_2 \approx 49\%$) to porphyritic monzonite ($SiO_2 \approx 53\%$) to syenite ($SiO_2 \approx 62\%$), with a gap at ~54%–60% SiO_2; a single compositionally layered sample of 57% SiO_2 may be a deformed example of magma mingling. Major and trace element compositions (Fig. 7) indicate that the Edwardsville pluton, located within the Adirondack Lowlands, is a member of the Frontenac suite. The Edwardsville pluton samples have moderate LREE enrichment (av. $La_n/Sm_n = 2.3$) and HREE depletion (av. $Sm_n/Yb_n = 3.2$), with small or no Eu anomalies (Fig. 7H), similar to plutons from the Frontenac suite.

The Beaver Creek pluton (Fig. 2) was called the Beaver Creek intrusive sheet by Buddington (1939) and the Huckleberry Mountain granite by Carl and deLorraine (1997), who noted similarities between the Beaver Creek pluton and the Rockport granite; however, in detail Beaver Creek pluton samples are more ferroan than the Rockport granite and have higher CaO contents at equivalent SiO_2 contents (cf. Figs. 5B and 7B and 5D and 7D). Geochemically the Beaver Creek pluton correlates well with the Frontenac suite (Fig. 7), and felsic samples (SiO_2 = 68%–75%) especially are very similar geochemically to samples from the Crow Lake, South Lake, and Perth Road plutons. Limited major element data for other syenite bodies in the Adirondack Lowlands (such as the Honey Hill pluton) suggest that they are also members of the Frontenac suite in the Adirondack Lowlands (Figs. 7A–7C).

Geochronology and Oxygen Isotopes of Zircon from Frontenac Igneous Suite Rocks in the Adirondack Lowlands

Two samples from the Edwardsville pluton and one from the Honey Hill pluton were selected for geochronology. Sample AGS-45 is an alkali-feldspar syenite from the northern part of the Edwardsville pluton, and is lithologically similar to the felsic sample of zircon dated by ID-TIMS as 1164 ± 4 Ma (McLelland et al., 1993). Elongate zircons (aspect ratios 1:2–1:4) were imaged using CL, and show oscillatory growth zoning with some minor sector or turbid zoning and occasional dark CL rims that truncate zoning (Fig. 9A). These textures are interpreted as magmatic features. Dating by SHRIMP-RG yielded relatively concordant analyses (Fig. 9B; Table 7), and $^{207}Pb/^{206}Pb$ ages that average 1187 ± 19 Ma (2σ, n = 12, mean square of weighted deviates, MSWD = 1.37). This sample has a zircon saturation temperature >1000 °C (after Watson and Harrison, 1983), predicting that inherited zircon should largely persist through anatexis and crystallization of this bulk composition. Ages of individual spots (with analytical uncertainties) yield essentially identical ages for cores and rims, with a range of ages that encompasses the ages of other Adirondack Lowlands suites; therefore, these ages reflect a maximum age of the magmatic origin of this pluton because of likely inheritance of igneous precursor zircon. We favor this interpretation based on the slightly younger 1164 ± 4 Ma age of McLelland et al. (1993) and the age of AGS-49 (following).

Sample AGS-49 is a monzonite collected from the southern part of the Edwardsville pluton. Zircon crystals separated from this sample have the shapes and CL zoning appearance of being fragments of originally large, anhedral crystals (Fig. 10A), similar to zircon commonly collected from mafic members of the AMCG suite elsewhere (McLelland et al., 2004). SHRIMP-RG analyses define a chord that intersects the concordia line at 1156 ± 49 Ma (2σ, n = 10, MSWD = 0.90). Discarding the two discordant spots, the regression intersects concordia at 1149 ± 22 Ma (Fig. 10B; 2σ, n = 8, MSWD = 0.56), which is our preferred age for this sample. The lack of textural evidence for zircon inheritance and this sample's mafic

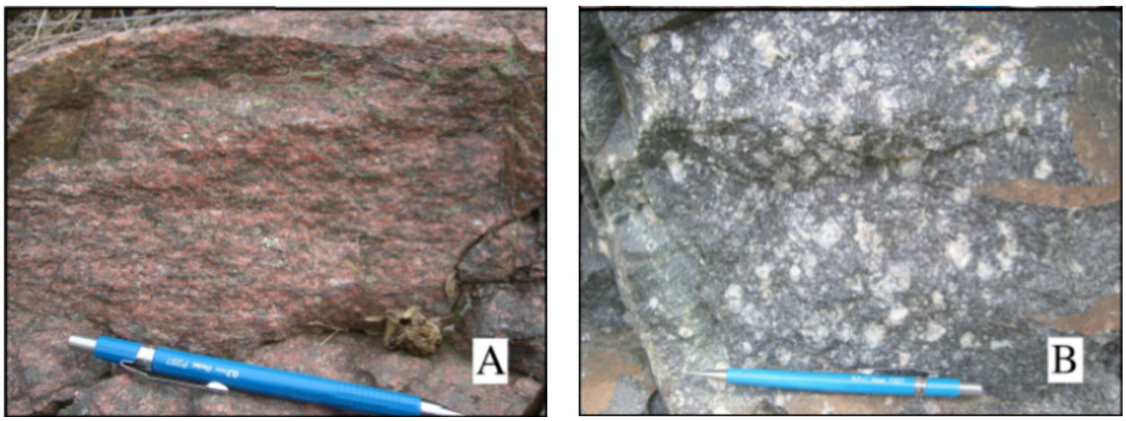

Figure 8. (A) Syenite of the Edwardsville pluton. (B) Porphyritic monzonite of the Edwardsville pluton. Pencil is ~20 cm long.

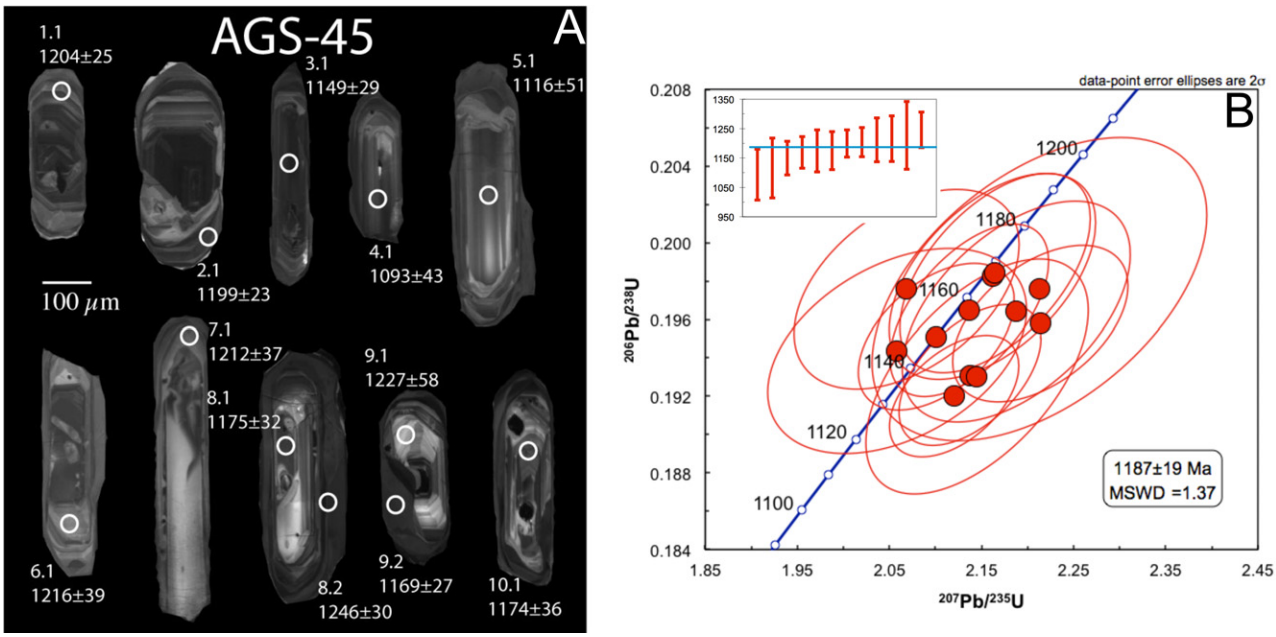

Figure 9. (A) Cathodoluminescence images of zircons from Edwardsville pluton sample AGS-45, dated by sensitive high-resolution ion microprobe–reverse geometry (SHRIMP-RG). $^{207}Pb/^{206}Pb$ ages of analytical spots and 2σ errors are shown (in Ma). (B) Concordia diagram of SHRIMP-RG analyses from AGS-45. Reported errors and ellipses are 2σ. Inset shows $^{207}Pb/^{206}Pb$ ages with 2σ errors of each analysis and average $^{207}Pb/^{206}Pb$ age shown as a horizontal line. MSWD—mean square of weighted deviates.

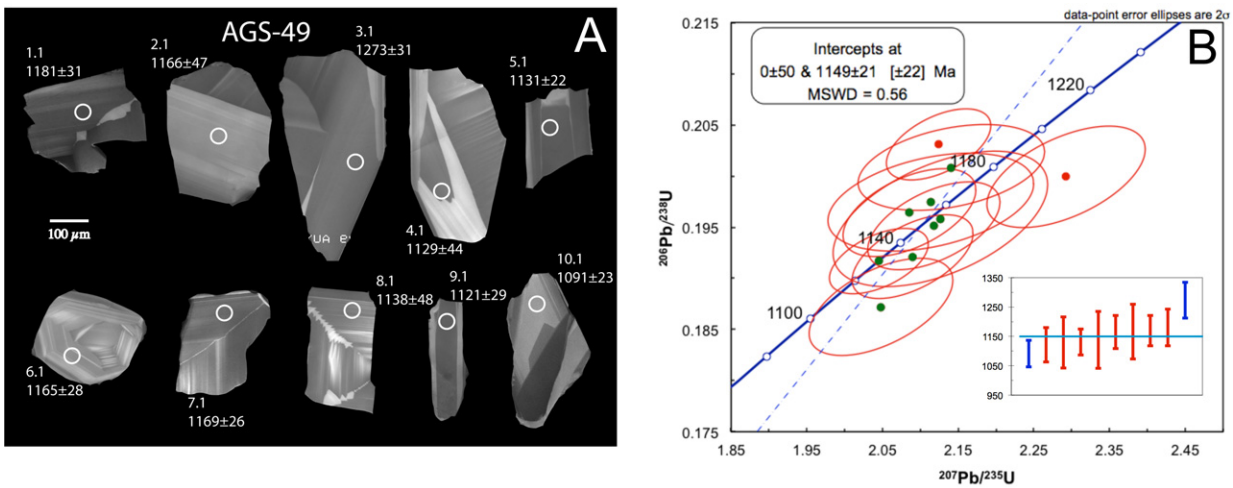

Figure 10. (A) Cathodoluminescence images of zircons from Edwardsville pluton sample AGS-49, dated by sensitive high-resolution ion microprobe–reverse geometry (SHRIMP-RG). $^{207}Pb/^{206}Pb$ ages of analytical spots and 2σ errors are shown (in Ma). (B) Concordia diagram of SHRIMP-RG analyses from AGS-49. Reported errors and ellipses are 2σ. Inset shows $^{207}Pb/^{206}Pb$ ages with 2σ errors of each analysis and average $^{207}Pb/^{206}Pb$ age shown as a horizontal line (spots excluded from dashed concordia regression are blue). MSWD—mean square of weighted deviates.

chemistry (indicating a zircon-undersaturated magma) make this age the best estimate for the magmatic age of the Edwardsville pluton, identical to the ages of other Frontenac suite plutons in Ontario.

The third rock selected for geochronology is a granitic sample (AGS-39) from the syenitic Honey Hill pluton mapped east of Red Lake by Buddington (1934). Zircons from this sample are similar to those from AGS-45, and six analyses concentrated on regions of oscillatory growth zoning away from cores or disturbed zoning (Fig. 11A). These spots define a cord that intersects the concordia line at 1161 ± 16 Ma (2σ, n = 6, MSWD = 0.62). One spot is 60% discordant and has 1449 ppm U. Discarding this point, the 5 remaining analyses have an average $^{207}Pb/^{206}Pb$ age of 1163 ± 16 Ma (2σ, n = 5, MSWD = 0.53), and a concordia age of 1165 ± 14 (2σ, n = 5, MSWD = 0.28). These ages are essentially identical, so we take the age of 1161 ± 16 Ma (the concordia age of all the points) to be the age of the Honey Hill pluton (Fig. 11B). This is similar to the age of other Frontenac suite plutons.

Oxygen isotope ratios in ca. 1155 Ma plutons are distinctively high for samples from the eastern Frontenac terrane ($\delta^{18}O_{zircon}$ = 11.8‰ ± 1.0‰ standard mean ocean water). The use of zircon for oxygen isotope analysis allows magmatic $\delta^{18}O$ to be calculated. For the Frontenac plutons, these values are 12.4‰–14.3‰, whereas values for AMCG plutons from the Adirondack Highlands are 7‰–9‰. These variations require fundamental differences in the lower crustal igneous source regions across the Adirondack Highlands–Adirondack Lowlands–Frontenac terrane–Sharbot Lake domain transect (Peck et al., 2004). The $\delta^{18}O_{zircon}$ from the dated Edwardsville pluton monzonite sample is 9.1‰, which is high for a mafic igneous rock, but considerably lower than isotope ratios found in Frontenac suite granitoids. Two felsic Edwardsville samples have very high $\delta^{18}O_{zircon}$ values of 11.2 (this study) and 11.1‰ (Peck et al., 2004), clearly indicating that it is part of the Frontenac suite. The difference in oxygen isotopes between the Edwardsville monzonite and syenite highlights the bimodal nature of the Frontenac suite plutons. Sample AGS-39 from the Honey Hill pluton has a high $\delta^{18}O_{zircon}$ of 9.9‰, which is also similar to the high $\delta^{18}O$ Frontenac suite. It is interesting that a fourth syenitic sample analyzed (AGS-15, from near Philadelphia, New York) has $\delta^{18}O_{zircon}$ = 8.0‰. This sample is from southeast of the Honey Hill body, and is lithologically similar and proximal to the 1155 Ma Diana complex, an AMCG pluton that is part of the boundary between the Adirondack Highlands and Adirondack Lowlands (Figs. 2 and 6). A sample from the Diana complex has $\delta^{18}O_{zircon}$ = 8.1‰ (Valley et al., 1994). These new data suggest that the transition from high $\delta^{18}O$ ($\delta^{18}O_{zircon}$ ≈ 10‰–12‰) to lower values ($\delta^{18}O_{zircon}$ ≈ 8‰) in the Adirondack Lowlands is to the east of the BLSZ, with the high $\delta^{18}O$ Honey Hill pluton being intermediate between values found in the Frontenac terrane and AGS-15 (Fig. 6). It is possible that the Honey Hill pluton may be derived from a mixture of high $\delta^{18}O$ lower crust to the west and lower $\delta^{18}O$ lower crust to the east that were tectonically mixed during the Shawinigan orogeny. A similar explanation may apply to the increased Nd T_{DM} model ages within the Antwerp-Rossie suite as the BLSZ is approached from the southeast (Chiarenzelli et al., 2010b).

Other Ferroan Magmatism in the Allochthonous Monocyclic Belt

The Frontenac terrane and Adirondack Lowlands continue to the north as the Central Metasedimentary Belt of Quebec, which contains country rock and intrusive suites similar to those in the Frontenac and Adirondack Lowlands terranes to the south (Corriveau and van Breemen, 2000). Rheologically rigid gneiss complexes in the Central Metasedimentary Belt are intruded by undeformed dioritic and monzonitic dikes of the 1.17–1.16 Ga Chevreuil suite.

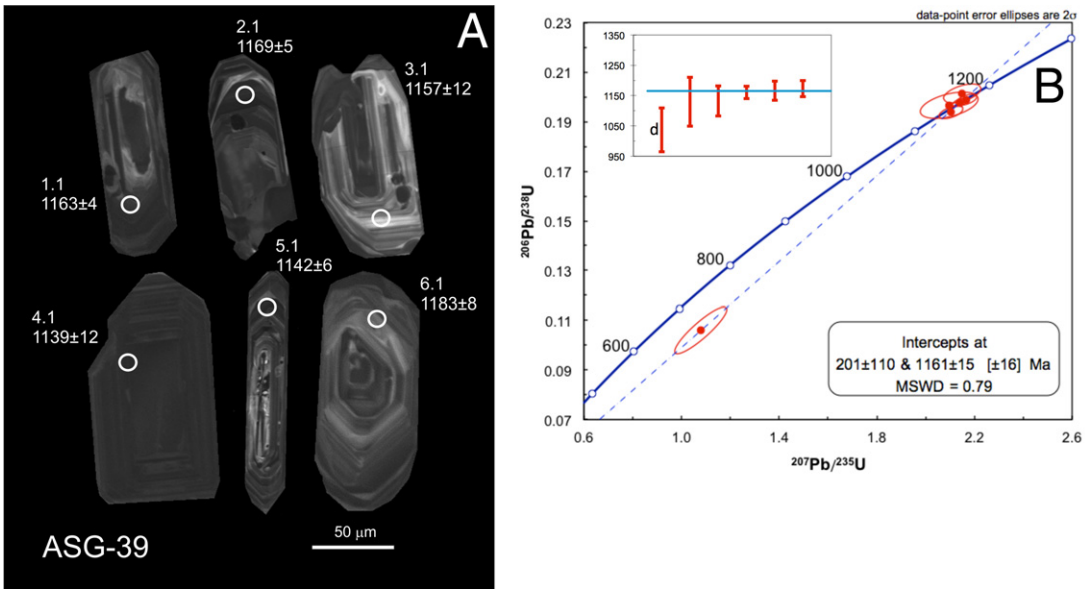

Figure 11. (A) Cathodoluminescence images of zircons from Honey Hill pluton sample AGS-39, dated by sensitive high-resolution ion microprobe–reverse geometry (SHRIMP-RG). $^{207}Pb/^{206}Pb$ ages of analytical spots and 2σ errors are shown (in Ma). (B) Concordia diagram of SHRIMP-RG analyses from AGS-39. Reported errors and ellipses are 2σ. Inset shows $^{207}Pb/^{206}Pb$ ages with 2σ errors of each analysis shown as a horizontal line. The average $^{207}Pb/^{206}Pb$ age (1163 ± 16 Ma) excludes the most discordant point (d), which is essentially the same age as the dashed concordia regression that includes all points. MSWD—mean square of weighted deviates.

The synkinematic monzonitic, dioritic, and gabbroic sheet-like plutons of this suite are preferentially emplaced into deformed metasedimentary rocks (Corriveau and van Breemen, 2000). Monzonite plutons of this suite are recognized east of the Labele shear zone (Fig. 1), where they intruded coevally with the 1.16–1.13 Ga anorthosite suite in the Morin terrane (Doig 1991; Corriveau and van Breemen, 2000). The western side of the Morin anorthosite massif is surrounded by a large body of ferrodiorite (jotunite) that grades into granitic rocks (mangerite). This body is distinct from the Chevreuil suite; it is metaluminous and has a calc-alkalic geochemical trend, while the Chevreuil suite both in the Central Metasedimentary Belt and Morin terrane is distinctly alkali-calcic and can be slightly peraluminous (Rockow, 1995; Corriveau, 2013). Oxygen isotopes of the Chevreuil suite monzonites and Morin mangerite are similar to each other ($\delta^{18}O_{zircon} \approx 7.5‰–9.5‰$), but high $\delta^{18}O$ values, such as those to the south in the Frontenac suite, were not observed (Peck et al., 2004). The Chevreuil suite lacks the strongly alkaline signature of the Frontenac suite (Fig. 12).

The Adirondack Highlands and Morin terranes are geologically similar; both are metamorphosed to the granulite facies, are dominated by metaplutonic rocks, and have similar thermal histories (Peck et al., 2005). In addition, anorthosites in the Adirondack Highlands and Morin terrane share oxygen isotope systematics that indicate substantial crustal contamination of parent magmas (Peck and Valley, 2000). Ferrodiorite to granitic rocks associated with the Adirondack Highlands anorthosite are for the most part alkalic to alkali-calcic in composition (intermediate between the Frontenac and Chevreuil suites) and are predominately metaluminous (Fig. 12; Seifert et al., 2010). Oxygen isotopes of these rocks ($\delta^{18}O_{zircon} \approx 8‰$; Valley et al., 1994) are similar to Chevreuil suite monzonites and Morin mangerite. The extent of the 1.17–1.15 Ga AMCG magmatism across several terrane boundaries and synkinematic intrusions into deformation zones in the allochthonous monocyclic belt indicates that these terranes had been juxtaposed by that time (Davidson and van Breemen, 2000; Corriveau and van Breemen, 2000).

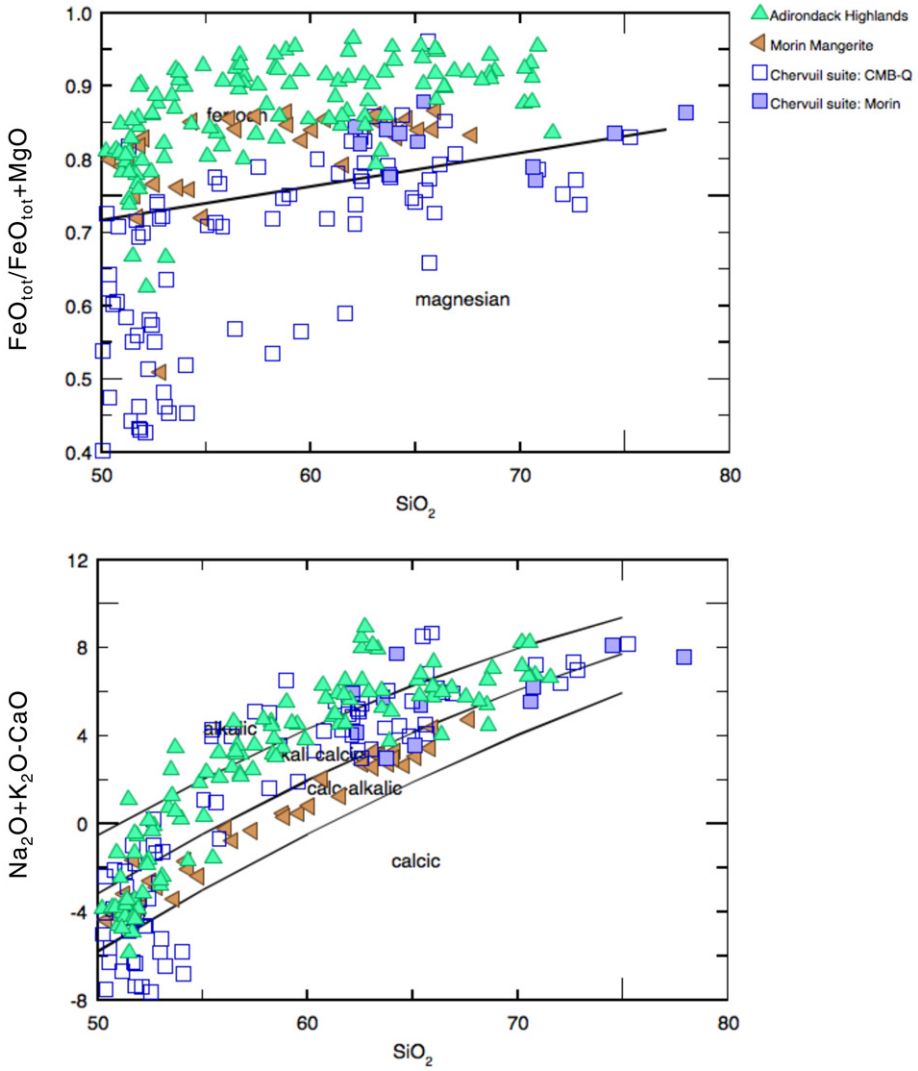

Figure 12. Discriminant diagrams for 1.15 Ga suites of the Central Metasedimentary Belt of Quebec (CMB-Q, Chevreuil suite), Morin mangerite, and mangerite-charnockite-granite suite of the Adirondack Highlands. Discriminant lines as in Figures 3B and 3C. Data are from Corriveau (2013), Rockow (1995), and Seifert et al. (2010).

Diverse Origin of Ferroan Magmatism in the Adirondack Lowlands and Frontenac Terrane

The geochemistry of magmatism in the Adirondack Lowlands progressed from bimodal magnesian and calc-alkalic (Antwerp-Rossie suite) to magnesian and alkalic to alkali-calcic to calc-alkalic (Hermon granite), through magnesian to ferroan and alkali-calcic–calc-alkalic (HSG and Rockport granite), and then to ferroan and strongly alkalic (Frontenac suite) during a period of ~50 m.y. (Fig. 3). The subduction-related Antwerp-Rossie suite magmatism is interpreted to have been formed during closure of a backarc basin between the Frontenac terrane and the Adirondack Highlands (Chiarenzelli et al., 2010b). The calc-alkaline Hermon granite may record the last melting event related to subduction during docking of these terranes, or perhaps subsequent collisional melting of mantle previously metasomatized during Antwerp-Rossie subduction, a feature seen in other collisional settings (e.g., Coulon et al., 2002). The syncollisional HSG and Rockport and postcollisional Frontenac suite magmatism are more alkalic than earlier magmas, and they have trace elements similar to other alkalic postcollisional suites elsewhere (e.g., Eby, 1992). Postcollisional magmatism with similar compositions has been ascribed to crustal delamination, creating a wide regional area of plutonism, or alternatively slab break-off, resulting in a structurally controlled and relatively narrow zone of melting (e.g., Tang et al., 2010). A delamination model is most consistent with the regional nature of ca. 1.15 Ga AMCG magmatism in the Adirondack Lowlands and the rest of the southern allochthonous monocyclic belt (e.g., McLelland et al., 2010a).

Most models for the origin of the AMCG suite previously invoked anorogenic or incipient rifting conditions (see Ashwal, 1993). We now

know that this is not likely because intrusion of AMCG rocks occurred during the terminal phase of, or just after, the Shawinigan orogeny in the Adirondacks (McLelland et al., 2010a). The vast volumes of massif anorthosite produced demands the influence of even greater volumes of mantle melts. To produce these melts, decompression melting of mantle peridotite is required, and models invoking delamination or detachment of the subducted slab and the rise of the asthenosphere have been proposed (McLelland et al., 2010a, 2010b; Regan et al., 2011). The nature of this mantle has recently been characterized by Nd isotopes and enriched geochemical traits of coronitic metagabbros. These primitive gabbros have a chemical composition nearly identical to enriched mid-oceanic ridge basalt (E-MORB) (Regan et al., 2011), distinct Nd systematics from other Adirondack metaigneous rocks, and occur as satellite plutons that intrude anorthosite and AMCG suite rocks. The coronitic gabbros were originally olivine bearing and were capable of crystallizing large volumes of plagioclase and olivine, which would drive the residual magmas toward Fe, Ti, and P enrichment. Numerous bodies of oxide- and oxide-apatite–rich gabbros are also associated with the massif anorthosites (Seifert et al., 2010), indicating the complementary magmatic residual products of anorthosite genesis. The distinct switch from a subduction-metasomatized mantle source to an enriched mantle occurred ca. 1170–1150 Ma, coincident with the end of the Shawinigan orogeny.

Origin of HSG and Rockport Granite

The Rockport granite and HSG emplacement at 1172 Ma occurred during the Shawinigan orogeny, which is interpreted as an effect of the crustal thickening and melting event caused by convergence and closure of the Trans-Adirondack basin (Fig. 3; Chiarenzelli et al., 2010b). The crust and intrusive suites in the allochthonous monocyclic belt are all relatively juvenile, having similar Nd isotope ratios. Thus, T_{DM} Nd model ages for the HSG and Rockport granite range from 1.2 to 1.4 Ga (McLelland et al., 1993), ages that overlap with those of the Antwerp-Rossie suite, Hermon granite, and Frontenac suite and the Adirondack metasediments they intruded, which are as young as 1.4 Ga (McLelland et al., 1996). Oxygen isotopes of the HSG and the Rockport granite are variable and range from $\delta^{18}O_{zircon}$ = 7.5‰ to 9.5‰ [$\delta^{18}O_{WR}$ (whole rock) ≈ 6.7‰–11.4‰; Valley et al., 2005], and bulk ID-TIMS clearly shows the contribution of zircons inherited from older evolved rocks (McLelland et al., 1991; Wasteneys et al., 1999). In addition, major and trace element geochemistry is consistent with the model by Wasteneys et al. (1999), that the HSG and Rockport granite are the product of melting a mixed amphibolite and granitoid crust that produced the tonalities and leucogranites, respectively, during the Shawinigan crustal thickening. This model explains the magnesian chemistry of the tonalitic phases of the HSG, peraluminous compositions in leucogranites, similarities in trace element geochemistry between these suites and the Antwerp-Rossie suite and Hermon granite, and the arc-like affinity of the HSG (McLelland et al., 1991). The Rockport granite gneisses are restricted to higher SiO_2 than HSG but have geochemically similar compositions. To illustrate how Rockport granite could be produced in this setting, the MELTS software package (Ghiorso and Sack 1995; Asimow and Ghiorso, 1998) was used to model melting during the Shawinigan orogeny. Melting was modeled using an average Antwerp-Rossie suite diorite composition as the source rock (51% SiO_2; Wasteneys et al. 1999), ~0.5% H_2O, and a progression of metamorphic temperatures extrapolated based on the current level of exposure from 850 °C and 7.5 kbar to 1050 °C and 9.5 kbar. This modeling produces a series of melts with SiO_2 = 62%–67% and K_2O = 4%–5% (Fig. 5), very similar to less evolved members of the Rockport granite (blue-gray facies; Carl and deLorraine, 1997) and consistent with the model of Wasteneys et al. (1999).

Origin of the Frontenac Suite and Other AMCG Granitoids

Anorthosite suite magmatism during 1.18–1.13 Ga spans several terranes of the allochthonous monocyclic belt. Granitoid members of the AMCG suite have distinct chemistry in different terranes, i.e., metaluminous and calc-alkalic jotunites and mangerites in the Morin terrane, the alkali-calcic Chevreuil suite, alkalic to alkali-calcic granitoids in the Adirondack Highlands, and the alkalic Frontenac suite. Because of the juvenile nature of the crust and the probable presence of enriched mantle beneath the allochthonous monocyclic belt in the Mesoproterozoic (Chiarenzelli et al., 2010a), Nd isotopes do not allow the proportions of crustal versus mantle components of these granitoids to be unambiguously calculated. However, there are other lines of evidence that point toward a large crustal component in the Frontenac suite and other anorthosite suite granitoids. For example, the 1.15 Ga ferroan granitoids from the Adirondack Highlands, with SiO_2 as low as 55%, have ca. 1.20 Ga or older inherited zircon (McLelland et al., 2004), suggesting that evolved crustal rocks were present at the site of origin of these melts. In addition, oxygen isotope compositions of these suites require substantial supracrustal contribution to parent magmas, further constraining AMCG origin (Valley et al., 1994; Peck et al., 2004).

Derivation of AMCG Granitoids from Tholeiites?

Frost and Frost (2011) proposed that ferroan granitoids associated with Proterozoic massif anorthosites are for the most part of two types: (1) alkalic metaluminous granitoids (often including rapakivi granites) interpreted as being the fractional crystallization products of mafic tholeiitic parent magmas, with little crustal involvement, and (2) alkali-calcic granitoids that are metaluminous to peraluminous and have larger crustal components. The Frontenac suite, which has anorthositic components in mafic plutons (Davidson and van Breemen, 2000), has some similarities to and some differences from with the first type. Unlike the ferroan alkalic batholiths in Wyoming (USA) or Norway, high SiO_2 Frontenac suite granites tend to be peraluminous and alkali-calcic, which may reflect crustal assimilation in evolved members of this suite (cf. Frost and Frost, 2011). However, oxygen isotope compositions of the Frontenac suite, especially the high-$\delta^{18}O$ plutons, are not simply the result of assimilation of country rocks (Peck et al., 2004) but require the melting of high-$\delta^{18}O$ source materials. To a lesser degree this is also the case for AMCG granitoids in the Adirondack Highlands (Fig. 13) and the Chevreuil suite and Morin mangerite, which have elevated $\delta^{18}O_{zircon}$ values (≥8‰) even for mafic members (Peck et al., 2004). Rocks derived from the mantle have a very limited range in $\delta^{18}O$; therefore, elevated $\delta^{18}O$ values in magmas are the result of origin from or assimilation of rocks that have undergone low-temperature interaction with the hydrosphere, i.e., sediments or hydrothermally altered rocks (Valley et al., 2005). All of these AMCG granitoids are elevated relative to mantle $\delta^{18}O_{zircon}$ values (5.5‰–6‰), and have trends of $\delta^{18}O$ versus SiO_2 that are consistent with source materials with elevated $\delta^{18}O$, and only limited $\delta^{18}O$ enrichment due to assimilation during fractional crystallization (Peck et al., 2004). An important aspect of the oxygen isotopic provinciality of the Frontenac suite is that there is no correlation of $\delta^{18}O$ with major, trace, or Nd isotope geochemistry either within the suite, or with contemporaneous ferroan granites from adjacent terranes. This relationship led to the conclusion (Peck et al., 2004) that the high-$\delta^{18}O$ Frontenac suite plutons were most likely caused by melting of underthrust hydrothermally altered ocean crust that, apart from its

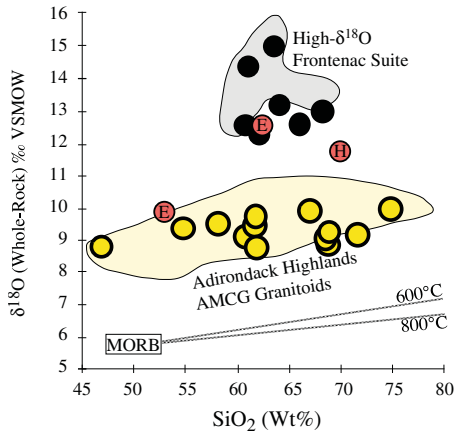

Figure 13. Oxygen isotope–silica diagram for the Frontenac suite, AMCG (anorthosite-mangerite-charnockite-granite) granitoids of the Adirondack Highlands, and (in red) new analyses from the Edwardsville (E) and Honey Hill (H) plutons. Circles are whole-rock values calculated from zircon after Peck et al. (2004) and Valley et al. (1994, 2005). Shaded fields encompass whole-rock analyses, which agree with those calculated from zircon. Lines show the effect of fractional crystallization from a MORB (mid-oceanic ridge basalt) starting composition, which cannot explain the oxygen isotopes of ferroan granites of the Frontenac suite of the Adirondack Highlands. VSMOW—Vienna standard mean ocean water.

high $\delta^{18}O$, was similar to MORB. Similar mechanisms have been proposed for the process by which radiogenically mantle-like tonalites with high $\delta^{18}O_{zircon}$ values formed in the Cretaceous Sierra Nevada batholith (Lackey et al., 2012).

The Fe- and K-rich chemistry of many ferroan granites, and their reduced oxidation state, has led some workers to invoke a mafic tholeiite as the ultimate source rocks (e.g., Frost and Frost, 1997; Frost et al., 1999). In this model, mafic magmas are produced by mantle melting below the base of the crust, followed by fractional crystallization in the crust along tholeiitic differentiation trends. Resulting gabbros or ferrodiorites are later melted in the lower crust to form the ferroan granites. This model can be generally applied to rocks of the Frontenac suite, except that the oxygen isotopes require that supracrustal materials play an important role. These constraints also apply to the AMCG granitoids in the Adirondack Highlands, Chevreuil suite, and Morin mangerite. Frost and Frost (1997) proposed that variable granite compositions can be caused by the proportions of melt from gabbros or ferrodiorites and felsic crust that is incorporated during anatexis in the lower crust. In this model, the most reduced rapakivi granites are most representative of melting of tholeiitic gabbros and ferrodiorites. Oxygen isotopes of some ferroan rapakivi granites seem to be consistent with this model, for example the Wolf River batholith (Wisconsin, USA), which has mantle-like $\delta^{18}O$ values (Kim, 1989; Valley et al., 2005). However, it is important to note that this is not always the case. For example, the reduced rapakivi Wiborg batholith in Finland and Russia, and other related rapakivi granite intrusions (Laitila, Ahvenisto, Suomenniemi) from north of the Porkkalaniemi shear zone, have elevated $\delta^{18}O$ values inconsistent with strictly mantle-derived sources (Elliott et al., 2005). The Finish granites have FeO_t (total iron)/(FeO_t + MgO) ≥ 0.92 and $\delta^{18}O_{WR}$ = 8.1‰–9.6‰ (calculated from zircon), which is elevated relative to mantle values. Hafnium isotope ratios (ε_{Hf}) of zircon from the Finish granites are relatively low at ~0, and also indicate mainly a crustal source (Heinonen et al., 2010), in agreement with the oxygen isotope data.

Relationship of Granitoids to Anorthosite Magmas

The association of anorthosites with related ferroan granitoids has been the topic of lively long-term debate. The controversy is focused on the extent to which granitoid magmas are differentiates of anorthosite or their parent magmas (see Ashwal, 1993). For example, McLelland et al. (2010b) outlined a now commonly cited scenario where postorogenic decompression causes mantle melting, and the melts pond and differentiate at the base of the crust (e.g., Heinonen et al., 2010). Buoyant crystal accumulations of plagioclase ascend and become anorthosite plutons, while melts of the lower crust (byproducts of mafic underplating) produce coeval granitoid plutons (Fig. 4). Another model (e.g., Vander Auwera et al., 1998) is that polybaric differentiation of ferrodiorite produces both anorthosite plutons and granitoid plutons. Oxygen isotope data bear on the viability of this model. Anorthosites from the allochthonous monocyclic belt have unusually high $\delta^{18}O$ values and are isotopically similar to associated granitoids, but most anorthosites elsewhere have mantle-like values, while associated granitoids are isotopically distinct (Peck and Valley, 2000; Peck et al., 2010). For example, in the Lac Allard Massif to the northeast of the allochthonous monocyclic belt, massif anorthosite is 1.6‰ lower than associated mangerite, more than can be attributed to fractional crystallization alone (Peck et al., 2010). Similar differences have been documented in the 1.4 Ga Laramie anorthosite complex (~1.7‰ difference; O'Connor and Morrison 1999) and the 1.4 Ga Kunene anorthosite in Namibia (~1.6‰ difference; Drüppel et al., 2007). Oxygen isotopes of anorthosite and granitoids from the Nain plutonic suite also preclude a straightforward comagmatic origin (Peck et al., 2010). The Nain anorthosite $\delta^{18}O_{WR}$ values range from 4.1‰ to 8.2‰, and show a clear dependence on location along a traverse across the Nain-Churchill province boundary (Archean-Proterozoic). Associated granitoids have $\delta^{18}O_{WR}$ values ranging from 7.4‰ to 8.8‰ that do not correlate with location. Granitic rocks with $\delta^{18}O$ values lower than associated anorthosites cannot be comagmatic because fractional crystallization causes increasing $\delta^{18}O$ in a magma series (Peck et al., 2004; Lackey et al., 2012). Isotope systematics also indicate that assimilants to Nain anorthosite parent magmas have different $\delta^{18}O$ than the source rocks for granitoids (Peck et al., 2010).

TECTONIC SUMMARY

The Adirondack Lowlands records a continuum of magmatism from 1.20 to 1.15 Ga caused by subduction, tectonic convergence, crustal thickening, and eventual orogenic collapse and melting of the lower crust. The 1.20 Ga bimodal Antwerp-Rossie suite magmatism was likely produced by subduction during closure of the Trans-Adirondack basin (Chiarenzelli et al., 2010b). The 1.18 Ga Hermon granite shares some of these arc-like geochemical signatures, but intruded during the beginning of crustal thickening and metamorphism caused by arc accretion and/or closure of basins during the Shawinigan orogeny. We interpret its geochemistry as reflecting melting of metasomatized mantle during convergence, essentially prolonging an arc-like magmatic signature after the end of subduction. Tectonically dismembered fragments of this altered mantle and oceanic crust (Pyrites complex) are now recognized in the Adirondack Lowlands (Chiarenzelli et al., 2010a, 2011b). At 1.17 Ga, intrusion of the HSG and the Rockport granite marked the transition from mantle melting to melting of crustal lithologies during the Shawinigan orogeny. This melting created a variety of magma compositions that intruded across the BLSZ, marking the amalgamation of the Adirondack Lowlands and Frontenac terrane at that time. Anorthosite suite magmatism began ca. 1.17 Ga and generated bimodal mafic and felsic magmas across the allochthonous monocyclic belt, with 1.15 Ga anorthosite massifs and granitoids intruding into the Adirondack Highlands and Morin terrane, and ferroan granitoid suites with lesser amounts of mafic magma intruding the Adirondack Lowlands and Frontenac terrane (Fronte-

nac suite) and Central Metasedimentary Belt (Chevreuil suite). Neodymium isotopes and trace element geochemistry of the 1.15 Ga gabbros in the Adirondack Highlands are consistent with upwelling of enriched asthenosphere causing anorthosite magmatism and heating of the lower crust (Regan et al., 2011), thought to be the result of postorogenic collapse and delamination of lithosphere after Shawinigan convergence (McLelland et al., 2010a). Oxygen isotopes of the Frontenac suite and other 1.15 Ga granitoids show a substantial high-$\delta^{18}O$ component and considerable variability across boundaries between assembled terranes, indicating that these lower crust melts were formed from the melting of supracrustal materials residing in the lower crust. These data contradict models that call for ferroan anorthosite suite granites to be primarily melts of underplated, mantle-derived (i.e., not supracrustal) material or differentiates of anorthosites or their parent magmas.

ACKNOWLEDGMENTS

We acknowledge the career of James McLelland and his encouragement of this research. Our work in the Adirondack Lowlands was made possible by support of the Keck Geology Consortium and by National Science Foundation (NSF) REU (Research Experiences for Undergraduates) grant 0648782. We thank Keck participants Isis Fukai, Steven Hochman, Josh Maurer, Robert Nowak, Ashley Russell, and Celina Will for their assistance in the field and laboratory. We also thank Ilya Bindeman (University of Oregon) and Joe Wooden (U.S. Geological Survey) for their assistance with analytical work and for hosting us in their laboratories. Some of the geochemistry of the Frontenac suite was generated by Kara Culgin, Jason Fredricks, Douglas Herling, Justin Kowalkoski, Molly Patterson, Jennifer Telling, Joshua Turka, Emmett Weatherford, and Michael Werner, who worked on these rocks as part of a class project in a petrology and analytical methods course at Colgate University (Hamilton, New York). We thank David Linsley, Di Keller, and Rebecca Tortorello at Colgate for their laboratory support. We thank the NSF for supporting instrumentation used for trace element analyses at Union College (Schenectady, New York; DUE-9952410). We also thank Bob Darling, two anonymous reviewers, and Graham Baird (the guest associate editor) for very thorough reviews of this work, and Dennis Harry for his editorial guidance.

REFERENCES CITED

Ashwal, L., 1993, Anorthosites: New York, Springer-Verlag, 422 p.

Asimow, P.D., and Ghiorso, M.S., 1998, Algorithmic modifications extending MELTS to calculate subsolidus phase relations: American Mineralogist, v. 83, p. 1127–1131.

Baird, G.B., and Shrady, C.H., 2011, Timing and kinematics of deformation in the northwest Adirondack Lowlands, New York State: Implications for terrane relationships in the southern Grenville Province: Geosphere, v. 7, p. 1303–1323, doi:10.1130/GES00689.1.

Bindeman, I., Gurenko, A., Sigmarsson, O., and Chaussidon, M., 2008, Oxygen isotope heterogeneity and disequilibria of olivine crystals in large volume Holocene basalts from Iceland: Evidence for magmatic digestion and erosion of Pleistocene hyaloclastites: Geochimica et Cosmochimica Acta, v. 72, p. 4397–4420, doi:10.1016/j.gca.2008.06.010.

Buddington, A.F., 1929, Granite phacoliths and their contact zones in northwest Adirondacks: New York State Museum Bulletin, v. 281, p. 51–107.

Buddington, A.F., 1934, Geology and mineral resources of the Hammond, Antwerp, and Lowville quadrangles: New York State Museum Bulletin, v. 296, 251 p.

Buddington, A.F., 1939, Adirondack igneous rocks and their metamorphism: Geological Society of America Memoir 7, 354 p., doi:10.1130/MEM7.

Carl, J.D., 2000, A geochemical study of amphibolite layers and other mafic rocks in the NW Adirondack Lowlands, New York: Northeastern Geology and Environmental Sciences, v. 22, p. 142–166.

Carl, J.D., and deLorraine, W.F., 1997, Geochemical and field characteristics of metamorphosed granitic rocks, NW Adirondack Lowlands, New York: Northeastern Geology and Environmental Science, v. 19, p. 276–301.

Carl, J.D., deLorraine, W.F., Mose, D.G., and Shieh, Y.N., 1990, Geochemical evidence for a revised Precambrian sequence in the Northwest Adirondacks, New York: Geological Society of America Bulletin, v. 102, p. 182–192, doi:10.1130/0016-7606(1990)102<0182:GEFARP>2.3.CO;2.

Carr, S., Easton, R.M., Jamieson, R.A., and Culshaw, N.G., 2000, Geologic transect across the Grenville orogen of Ontario and New York: Canadian Journal of Earth Sciences, v. 37, p. 193–216, doi:10.1139/e99-074.

Chiarenzelli, J., Lupulescu, M., Cousens, B., Thern, E., Coffin, L., and Regan, S., 2010a, Enriched Grenvillian lithospheric mantle as a consequence of long-lived subduction beneath Laurentia: Geology, v. 38, p. 151–154, doi:10.1130/G30342.1.

Chiarenzelli, J., Regan, S., Peck, W.H., Selleck, B.W., Cousens, B., Baird, G.B., and Shrady, C.H., 2010b, Shawinigan arc magmatism in the Adirondack Lowlands as a consequence of closure of the Trans-Adirondack backarc basin: Geosphere, v. 6, p. 900–916, doi:10.1130/GES00576.1.

Chiarenzelli, J., Hudson, M., Dahl, P., and deLorraine, W.D., 2011a, Constraints on deposition in the Trans-Adirondack Basin, northern New York: Composition and origin of the Popple Hill Gneiss: Precambrian Research, v. 214–215, p. 154–171, doi:10.1016/j.precamres.2011.10.024.

Chiarenzelli, J., Lupulescu, M., Thern, E., and Cousens, B., 2011b, Tectonic implications of the discovery of a Shawinigan ophiolite (Pyrites Complex) in the Adirondack Lowlands: Geosphere, v. 7, p. 333–356, doi:10.1130/GES00608.1.

Corrigan, D., and Hanmer, S., 1997, Anorthosites and related granitoids in the Grenville orogen: A product of convective thinning of the lithosphere?: Geology, v. 25, p. 61–64, doi:10.1130/0091-7613(1997)025<0061:AARGIT>2.3.CO;2.

Corriveau, L., 2013, Architecture de la ceinture métasédimentaire centrale au Québec, Province de Grenville: Un exemple de l'analyse de terrains de métamorphisme élevé: Commission Géologique du Canada Bulletin 586, 264 p.

Corriveau, L., and van Breemen, O., 2000, Docking of the Central Metasedimentary Belt to Laurentia in geon 12: Evidence from the 1.17–1.16 Ga Chevreuil intrusive suite and host gneisses, Quebec: Canadian Journal of Earth Sciences, v. 37, p. 253–269, doi:10.1139/e00-004.

Corriveau, L., and Leblanc, D., 1995, Sequential nesting of magmas in marble, SW Grenville province: From fracture propagation to diapirism: Tectonophysics, v. 246, p. 183–200, doi:10.1016/0040-1951(94)00265-B.

Coulon, C., Fourcade, S., Maury, R.C., Bellon, H., Louni-Hacini, A., Cotten, J., Coutelle, A., and Hermitte, D., 2002, Post-collisional transition from calc-alkaline to alkaline volcanism during the Neogene in Oranie (Algeria): Magmatic expression of a slab breakoff: Lithos, v. 62, p. 87–110, doi:10.1016/S0024-4937(02)00109-3.

Currie, K.L., and Ermanovics, I.F., 1971, Geology of the Loughborough Lake region, Ontario, with a special emphasis on the origin of granitoid rocks: Geological Survey of Canada Bulletin 199, 71 p.

Davidson, A., 1996, Post-collisional A-type plutonism, southwest Grenville Province: Evidence for a compressional setting: Geological Society of America Abstracts with Programs, v. 28, no. 7, p. 440.

Davidson, A., and van Breemen, O., 2000, The age and extent of the Frontenac plutonic suite in the Central Metasedimentary Belt, Grenville Province, Ontario: Radiogenic age and isotope studies report 13: Geological Survey of Canada Current Research 2000–F4, 15 p.

Dickin, A.P., and McNutt, R.H., 2007, The Central Metasedimentary Belt (Grenville Province) as a failed back-arc rift zone: Nd isotope evidence: Earth and Planetary Science Letters, v. 259, p. 97–106, doi:10.1016/j.epsl.2007.04.031.

Doig, R., 1991, U-Pb zircon dates of Morin anorthosite suite rocks, Grenville Province, Quebec: Journal of Geology, v. 99, p. 729–738, doi:10.1086/629535.

Drüppel, K., Littmann, S., Romer, R.L., and Okrusch, M., 2007, Petrology and isotope geochemistry of the Mesoproterozoic anorthosite and related rocks of the Kunene Intrusive Complex, NW Namibia: Precambrian Research, v. 156, p. 1–31.

Eby, G.N., 1992, Chemical subdivision of the A-type granitoids: Petrogenetic and tectonic implications: Geology, v. 20, p. 641–644, doi:10.1130/0091-7613(1992)020<0641:CSOTAT>2.3.CO;2.

Elliott, B.A., Peck, W.H., Rämö, O.T., and Vaasjoki, M., 2005, Magmatic zircon oxygen isotopes of 1.88–1.87 Ga orogenic and 1.85–154 Ga anorogenic magmatism in Finland: Mineralogy and Petrology, v. 85, p. 223–241, doi:10.1007/s00710-005-0087-3.

Ermanovics, I.F., 1970, Zonal structure of the Perth Road monzonite, Grenville Province, Ontario: Canadian Journal of Earth Sciences, v. 7, p. 414–434, doi:10.1139/e70-036.

Fischer, J.C., 1995, Field and geochemical study of amphibolites of basic dikes of the Hyde School and Fish Creek Bodies of the Hyde School Gneiss, Adirondack Lowlands, New York [M.S. thesis]: Oxford, Ohio, Miami University, 173 p.

Fisher, D.W., Isachsen, Y.W., and Rickard, L.V., 1970, Geologic map of New York: New York State Museum and Science Service Map and Chart Series, no. 15, scale 1:250,000.

Frost, C.D., and Frost, B.R., 1997, Reduced rapakivi-type granites: The tholeiite connection: Geology, v. 25, p. 647–650, doi:10.1130/0091-7613(1997)025<0647:RRTGTT>2.3.CO;2.

Frost, B.R., and Frost, C.D., 2008, Geochemical classification for feldspathic igneous rocks: Journal of Petrology, v. 49, p. 1955–1969, doi:10.1093/petrology/egn054.

Frost, C.D., and Frost, B.R., 2011, On ferroan (A-type) granitoids: Their compositional variability and modes of origin: Journal of Petrology, v. 52, p. 39–53, doi:10.1093/petrology/egq070.

Frost, C.D., Frost, B.R., Chamberlain, K.R., and Edwards, B.R., 1999, Petrogenesis of the 1.43 Ga Sherman batholith, SE Wyoming, USA: A reduced, rapakivi-type anorogenic granite: Journal of Petrology, v. 40, p. 1771–1802.

Ghiorso, M.S., and Sack, R.O., 1995, Chemical mass transfer in magmatic processes. IV. A revised and internally consistent thermodynamic model for the interpolation and extrapolation of liquid-solid equilibria in magmatic systems at elevated temperatures and pressures: Contributions to Mineralogy and Petrology, v. 119, p. 197–212, doi:10.1007/BF00307281.

Grammatikopoulos, A., Clark, A., and Archibald, D., 2007, Petrogenesis of the Leo Lake and Lyndhurst plutons, Frontenac terrane, Central Metasedimentary Belt, southeastern Ontario, Canada: Canadian Journal of Earth Sciences, v. 44, p. 107–126, doi:10.1139/e06-072.

Hamilton , M.A., McLelland, J.M., and Selleck, B.W., 2004, SHRIMP U/Pb zircon geochronology of the anorthosite-mangerite-charnockite-granite suite, Adirondack Mountains, New York: Ages of emplacement and metamorphism, *in* Tollo, R.P., et al., eds., Proterozoic tectonic evolution of the Grenville orogen in North America: Geological Society of America Memoir 197, p. 337–355, doi:10.1130/0-8137-1197-5.337.

Hanmer, S., Corrigan, D., Pehrsson, S. and Nadeau, L., 2000, SW Grenville Province, Canada: The case against post-1.4 Ga accretionary tectonics: Tectonophysics, v. 319, p. 33–51, doi:10.1016/S0040-1951(99)00317-0.

Harpp, K.S., Wanless, V.D., Otto, R.H., Hoernle, K., and Werner, R., 2005, The Cocos and Carnegie aseismic ridges: A trace element record of long-term plume–spreading center interaction: Journal of Petrology, v. 46, p. 109–133, doi:10.1093/petrology/egh064.

Heinonen, A.P., Andersen, T., and Rämö, O.T., 2010, Re-evaluation of rapakivi petrogenesis: Source constraints from the Hf isotope composition of zircon in the rapakivi granites and associated mafic rocks of southern Finland: Journal of Petrology, v. 51, p. 1687–1709, doi:10.1093/petrology/egq035.

Heumann, M.J., Bickford, M., Hill, B.M., McLelland, J.M., Selleck, B.W., and Jercinovic, M.J., 2006, Timing of anatexis in metapelites from the Adirondack lowlands and southern highlands: A manifestation of the Shawinigan orogeny and subsequent anorthosite-mangerite-charnockite-granite magmatism: Geological Society of America Bulletin, v. 118, p. 1283–1298, doi:10.1130/B25927.1.

Hollocher, K., Robinson, P., Walsh, E., and Terry, M., 2007, The Neoproterozoic Ottfjället dike swarm of the Middle Allochthon, traced geochemically into the Scandian Hinterland, Western Gneiss Region, Norway: American Journal of Science, v. 307, p. 901–953, doi:10.2475/06.2007.02.

Hudson, R.M., 1994, P-T-X-t constraints on ductile deformation zones within the Adirondack Lowlands [Ph.D. thesis]: Oxford, Ohio, Miami University 194 p.

Irvine, T., and Baragar, W., 1971, A guide to the chemical classification of the common volcanic rocks: Canadian Journal of Earth Sciences, v. 8, p. 523–548.

Kim, S.-J., 1989, Oxygen and sulfur isotope studies of the Wolf River Batholith in Wisconsin and related Precambrian anorogenic granitic rocks in the midcontinent of North America [Ph.D. Thesis]: West Lafayette, Indiana, Purdue University, 199 p.

Lackey, J.S., Cecil, M.R., Windham, C.J., Frazer, R.E., Bindeman, I.N., and Gehrels, G., 2012, The Fine Gold Intrusive Suite: The roles of basement terranes and magma source development in the Early Cretaceous Sierra Nevada batholith: Geosphere, v. 8, p. 292–313, doi:10.1130/GES00745.1.

Ludwig, K.R., 2001, Squid 1.02: A user's manual: Berkeley, California, Berkeley Geochronology Center Special Publication 2, 19 p.

Ludwig, K.R., 2008, Isoplot 3.7: A geochronological toolkit for Microsoft Excel: Berkeley, California, Berkeley Geochronology Center Special Publication 4, 77 p.

Maher, T.M., 1981, Rb-Sr systematic and rare-earth geochemistry of Precambrian leucogneisses from the Adirondack Lowlands, NY [M.S. thesis]: Oxford, Ohio, Miami University, 127 p.

Marcantonio, F., McNutt, R.H., Dickin, A.P., and Heaman, L.M., 1990, Isotopic evidence for the crustal evolution of the Frontenac Arch in the Grenville Province of Ontario, Canada: Chemical Geology, v. 83, p. 297–314, doi:10.1016/0009-2541(90)90286-G.

McLelland, J., Chiarenzelli, J., and Perham, A., 1991, Age, field, and petrological relationships of the Hyde School Gneiss, Adirondack Lowlands, New York: Criteria for an intrusive origin: Journal of Geology, v. 100, p. 69–90, doi:10.1086/629572.

McLelland, J., Daly, J.S., and Chiarenzelli, J., 1993, Sm-Nd and U-Pb isotopic evidence for Juvenile crust in the Adirondack Lowlands and implications for the evolution of the Adirondack Mts.: Journal of Geology, v. 101, p. 97–105, doi:10.1086/648198.

McLelland, J.M., Daly, J.S., and McLelland, J.M., 1996, The Grenville orogenic cycle (ca. 1350–1000 Ma): An Adirondack perspective: Tectonophysics, v. 265, p. 1–28, doi:10.1016/S0040-1951(96)00144-8.

McLelland, J.M., Bickford, M.E., Hill, B.M., Clechenko, C.C., Valley, J.W., and Hamilton, M.A., 2004, Direct dating of Adirondack massif anorthosite by U-Pb SHRIMP analysis of igneous zircon: Implications for AMCG complexes: Geological Society of America Bulletin, v. 116, p. 1299–1317, doi:10.1130/B25482.1.

McLelland, J.M., Selleck, B.W., and Bickford, M.E., 2010a, Review of the Proterozoic evolution of the Grenville Province, its Adirondack outlier, and the Mesoproterozoic inliers of the Appalachians, *in* Tollo, R.P., et al., eds., From Rodinia to Pangea: The lithotectonic record of the Appalachian region: Geological Society of America Memoir 206, p. 21-49, doi:10.1130/2010.1206(02).

McLelland, J.M., Selleck, B.W., Hamilton, M.A., and Bickford, M.E., 2010b, Late- to post-tectonic setting of some major Proterozoic anorthosite-mangerite-charnockite-granite (AMCG) suites: Canadian Mineralogist, v. 48, p. 729–750, doi:10.3749/canmin.48.4.729.

Mezger, K., Rawnsley, C.M., Bohlen, S.R., and Hanson, G.N., 1991, U-Pb garnet, sphene, monazite, and rutile ages: Implications for the duration of high grade metamorphism and cooling histories, Adirondack Mts., New York: Journal of Geology, v. 99, p. 415–428, doi:10.1086/629503.

Mezger, K., Essene, E.J., van der Pluijm, B.A., and Halliday, A.N., 1993, U-Pb geochronology of the Grenville Orogen of Ontario and New York: Constraints on ancient crustal tectonics: Contributions to Mineralogy and Petrology, v. 114, p. 13–26, doi:10.1007/BF00307862.

O'Connor, Y.-L. and Morrison, J., 1999, Oxygen isotope constraints on the petrogenesis of the Sybille intrusion of the Proterozoic Laramie Anorthosite Complex: Contributions to Mineralogy and Petrology, v. 136, p. 81–91.

Pearce, J.A., Harris, N.B.W., and Tindle, A.G., 1984, Trace element discrimination diagrams for tectonic interpretations of granitic rocks: Journal of Petrology, v. 25, p. 956–983, doi:10.1093/petrology/25.4.956.

Pearce, J.A., Bender, J.F., De Long, S.E., Kidd, W.S.F., Low, P.J., Guner, Y., Saroglu, F., Yilmaz, Y., Moorbath, S., and Mitchell, J.G., 1990, Genesis of collision volcanism in eastern Anatolia, Turkey: Journal of Volcanology and Geothermal Research, v. 44, p. 189–229, doi:10.1016/0377-0273(90)90018-B.

Peck, W.H., and Valley, J.W., 2000, Large crustal input to high $\delta^{18}O$ anorthosite massifs of the southern Grenville Province: New evidence from the Morin Complex, Quebec: Contributions to Mineralogy and Petrology, v. 139, p. 402–417, doi:10.1007/s004100000149.

Peck, W.H., Valley, J.W., Corriveau, L., Davidson, A., McLelland, J., and Farber, D.A., 2004, Oxygen-isotope constraints on terrane boundaries and origin of 1.18–1.13 Ga granitoids in the southern Grenville Province, *in* Tollo, R.P., et al., eds., Proterozoic tectonic evolution of the Grenville orogen in North America: Geological Society of America Memoir 197, p. 163–182, doi:10.1130/0-8137-1197-5.163.

Peck, W.H., DeAngelis, M.T., Meredith, M.T., and Morin, E., 2005, Polymetamorphism of marbles in the Morin terrane (Grenville Province, Quebec): Canadian Journal of Earth Sciences, v. 42, p. 1949–1965, doi:10.1139/e05-070.

Peck, W.H., Clechenko, C.C., Hamilton, M.A., and Valley, J.W., 2010, Oxygen isotopes in the Grenville and Nain AMCG Suites: Regional aspects of the crustal component in massif anorthosites: Canadian Mineralogist, v. 48, p. 763–786, doi:10.3749/canmin.48.4.763.

Peck, W.H., Selleck, B.W., and Wong, M.S., 2011, Geology of the Black Lake shear zone and Northwestern Adirondack Lowlands, Grenville Province, New York: Friends of the Grenville Annual Field Trip, September 10–11, 2011, Alexandria Bay, N.Y.: Hamilton, New York, Colgate University Department of Geology, 63 p.

Premo, W.R., Castineiras, P., and Wooden, J.L., 2008, SHRIMP-RG U-Pb isotopic systematics of zircon from the Angel Lake orthogneiss, east Humboldt Range, Nevada: Is this really Archean crust?: Geosphere, v. 4, p. 963–975, doi:10.1130/GES00164.1.

Regan, S.P., Chiarenzelli, J.R., McLelland, J.M., and Cousens, B.L., 2011, Evidence for an enriched asthenospheric source for coronitic metagabbros in the Adirondack Highlands: Geosphere, v. 7, p. 694–709, doi:10.1130/GES00629.1.

Rivers, T., Martignole, J., Gower, C.F., and Davidson, A., 1989, New tectonic divisions of the Grenville Province, southeast Canadian Shield: Tectonics, v. 8, p. 63–84, doi:10.1029/TC008i001p00063.

Rockow, M.W., 1995, Petrogenesis of the jotunite unit at the Morin Complex, Grenville Province, Quebec: A field, mineralogical, and chemical study [Ph.D. thesis]: St. Louis, Missouri, Washington University, 477 p.

Seifert, K.E., Dymek, R.F., Whitney, P.R., and Haskin, L.A., 2010, Geochemistry of massif anorthosite and associated rocks, Adirondack Mountains, New York: Geosphere, v. 6, p. 855–899, doi:10.1130/GES00550.1.

Selleck, B.W., McLelland, J.M., and Bickford, M.E., 2005, Granite emplacement during tectonic exhumation: The Adirondack example: Geology, v. 33, p. 781–784, doi:10.1130/G21631.1.

Streepey, M.M., Essene, E.J., and van der Pluijm, B.A., 1997, A compilation of thermobarometric data from the metasedimentary belt of the Grenville Province, Ontario and New York State: Canadian Mineralogist, v. 35, p. 1237–1247.

Sun, S.S., and McDonough, W.F., 1989, Chemical and isotopic systematics of oceanic basalts: Implications for mantle composition and processes, *in* Saunders, A.D., and Norry, M.J., eds., Magmatism in the ocean basins: Geological Society of London Special Publication 42, p. 313–345, doi:10.1144/GSL.SP.1989.042.01.19.

Tang, G.-J., Wang, Q., Zhao, Z.-H., Sun, W.-D., Jia, X.-H., Jiang, Z.-Q., Li, Z.-X., Wyman, D.A., and Sun, M., 2010, Geochronology and geochemistry of late Paleozoic magmatic rocks in the Lamasu-Dabate area, northwestern Tianshan (west China): Evidence for a tectonic transition from arc to post-collisional setting: Lithos, v. 119, p. 393–411, doi:10.1016/j.lithos.2010.07.010.

Till, C.B., Gans, P.B., Spera, F.J., MacMillan, I., and Blair, K.D., 2009, Perils of petrotectonic modeling: A view from southern Sonora, Mexico: Journal of Volcanology and Geothermal Research, v. 186, p. 160–168, doi:10.1016/j.jvolgeores.2009.06.014.

Valley, J.W., Chiarenzelli, J.R., and McLelland, J.M., 1994, Oxygen isotope geochemistry of zircon: Earth and Planetary Science Letters, v. 126, p. 187–206, doi:10.1016/0012-821X(94)90106-6.

Valley, J.W., Kitchen, N., Kohn, M.J., Niendorf, C.R., and Spicuzza, M.J., 1995, UWG-2, a garnet standard for oxygen isotope ratio: Strategies for high precision and accuracy with laser heating: Geochimica et Cosmochimica Acta, v. 59, p. 5223–5231, doi:10.1016/0016-7037(95)00386-X.

Valley, J.W., and 12 others, 2005, 4.4 billion years of years of crustal maturation: Oxygen isotope ratios of magmatic zircon: Contributions to Mineralogy and Petrology, v. 150, p. 561–580, doi:10.1007/s00410-005-0025-8.

van Breemen, O., and Davidson, A., 1988, U-Pb zircon ages of granites and syenites in the Central Metasedimentary Belt, Grenville Province, Ontario, *in* Radiogenic age and isotopic studies, issue 2: Geological Survey of Canada Paper 88–2, p. 45–50.

Vander Auwera, J., Longhi, J., and Duchesne, J. C., 1998, A liquid line of descent of the jotunite (hypersthene monzodiorite) suite: Journal of Petrology, v. 39, p. 439–468.

Wasteneys, H., McLelland, J., and Lumbers, S., 1999, Precise zircon geochronology in the Adirondack Lowlands and implications for revising plate tectonic models of the Central Metasedimentary Belt and Adirondack Mountains, Grenville Province, Ontario and New York: Canadian Journal of Earth Sciences, v. 36, p. 967–984, doi:10.1139/e99-020.

Watson, E.B., and Harrison, T.M., 1983, Zircon saturation revisited: Temperature and composition effects in a variety of crustal magma types: Earth and Planetary Science Letters, v. 64, p. 295–304, doi:10.1016/0012-821X(83)90211-X.

Whalen, J.B., Currie, K.L., and Chappel, B.W., 1987, A-type granites: Geochemical characteristics, discriminations and petrogenesis: Contributions to Mineralogy and Petrology, v. 95, p. 407–419, doi:10.1007/BF00402202.

Wiener, R.W., McLelland, J.M., Isachesen, Y.W., and Hall, L.M., 1984, Stratigraphy and structural geology of the Adirondack Mountains, New York: Review and synthesis, *in* Bartholomew, M.J., ed., The Grenville event in the Appalachians and related topics: Geological Society of America Special Paper 194, p. 1–55.

Wong, M.S., Peck, W.H., Selleck, B.W., Catalano, J.P., Hochman, S.D., and Maurer, J.T., 2011, The Black Lake Shear Zone: A boundary between terranes in the Adirondack Lowlands, Grenville Province: Precambrian Research, v. 188, p. 57–72, doi:10.1016/j.precamres.2011.04.001.